

# A review on theoretical models for lithium–sulfur battery cathodes

Shuai Feng<sup>1</sup>  | Zhong-Heng Fu<sup>2</sup>  | Xiang Chen<sup>2</sup>  | Qiang Zhang<sup>2</sup> 

<sup>1</sup>College of Chemistry and Chemical Engineering, Taishan University, Tai'an, China

<sup>2</sup>Beijing Key Laboratory of Green Chemical Reaction Engineering and Technology, Department of Chemical Engineering, Tsinghua University, Beijing, China

## Correspondence

Xiang Chen and Qiang Zhang, Beijing Key Laboratory of Green Chemical Reaction Engineering and Technology, Department of Chemical Engineering, Tsinghua University, Beijing 100084, China.  
Email: xiangchen@mails.tsinghua.edu.cn and zhang-qiang@mails.tsinghua.edu.cn

## Funding information

Beijing Municipal Natural Science Foundation, Grant/Award Number: Z200011; National Natural Science Foundation of China, Grant/Award Numbers: 22109086, 21825501; Tai'an Municipal Technology Foundation, Grant/Award Number: 2019GX049

## Abstract

Lithium–sulfur (Li–S) batteries have been considered as promising battery systems due to their huge advantages on theoretical energy density and rich resources. However, the shuttle effect and sluggish transformation of soluble lithium polysulfides (LiPSs) hinder the practical application of Li–S batteries. Tremendous sulfur host materials with unique catalytic activity have been exploited to inhibit the shuttle effect and accelerate LiPSs redox reactions, in which theoretical simulations have been widely adopted. This review aims to summarize the fundamentals and applications of theoretical models in sulfur cathodes. Concretely, the integration of theoretical models provides insights into the adsorption and conversion mechanisms of LiPSs and is further utilized in the smart design of catalysts for the exploitation of practical Li–S batteries. Finally, a perspective on the future combination of calculation technology and theoretical models is provided.

## KEY WORDS

DFT calculations, electrocatalysts, Li–S batteries, sulfur cathodes, theoretical models

## 1 | INTRODUCTION

With the ever-increasing demand for utilizing renewable energy, advanced energy storage devices have been highly required to be more environmentally friendly and economical.<sup>1–10</sup> Li–S battery is one of the most promising candidates among various battery systems due to their ultrahigh theoretical energy density of 2600 Wh kg<sup>−1</sup>.<sup>11–18</sup> More importantly, the cathode materials, elemental sulfur, afford profitable features like natural abundance, environmental friendliness, and low cost.<sup>19–22</sup> However, there remain several drawbacks for Li–S batteries especially for the cathode, which severely hinders their practical

applications.<sup>23,24</sup> Specifically, the low electrical conductivity of sulfur ( $10^{-7}$  to  $10^{-30}$  S cm<sup>−1</sup> at room temperature) and the insulating nature of sulfur as well as its discharge products (Li<sub>2</sub>S or Li<sub>2</sub>S<sub>2</sub>) render it deficient to be directly applied as the cathode.<sup>25</sup> Volume expansion of the electrode (~80%) is also an imperative issue originating from the different volumetric densities of S<sub>8</sub> and Li<sub>2</sub>S.<sup>17</sup> More seriously, the notorious “polysulfide shuttle effect” not only induces a self-discharge but also corrodes lithium metal anodes and consequently causes rapid capacity degradation.<sup>26–28</sup>

Recently, tremendous efforts have been devoted to handling these disastrous issues facing Li–S batteries,

This is an open access article under the terms of the Creative Commons Attribution License, which permits use, distribution and reproduction in any medium, provided the original work is properly cited.

© 2022 The Authors. *InfoMat* published by UESTC and John Wiley & Sons Australia, Ltd.

especially the “shuttle effect”.<sup>29–41</sup> Conductive carbon materials, like 0D carbon capsules,<sup>42</sup> 1D carbon nanotubes,<sup>43</sup> 2D graphene nanosheets,<sup>22</sup> and 3D porous graphitic carbon,<sup>44,45</sup> were preferentially chosen to modulate the behaviors of LiPSs through van der Waals force and finite space effect. However, the weak interaction between carbon materials and LiPSs cannot effectively impede the shuttle of LiPSs. Subsequently, a variety of strategies were further proposed to modify carbon materials, that is, introducing heteroatoms (N, O, P, B, S, etc.)<sup>46–48</sup> or surface functionalization groups (—OH, —O functional groups, etc.) to immobilize LiPSs.<sup>49</sup> Moreover, polar compounds (such as layered double hydroxides [LDHs], metal oxides, and metal sulfides<sup>50–52</sup>) become promising alternatives as sulfur host materials due to their strong adsorption with LiPSs. As the understanding of the working mechanism deepens, the sluggish kinetics of sulfur reduction reaction (SRR) on the cathode has been widely confirmed as the bottleneck in achieving high-performance Li–S batteries.<sup>53–56</sup> Therefore, the priority has switched from anchoring LiPSs in cathode frameworks to promoting the conversion between LiPSs and Li<sub>2</sub>S<sub>x</sub>/Li<sub>2</sub>S.<sup>57–59</sup>

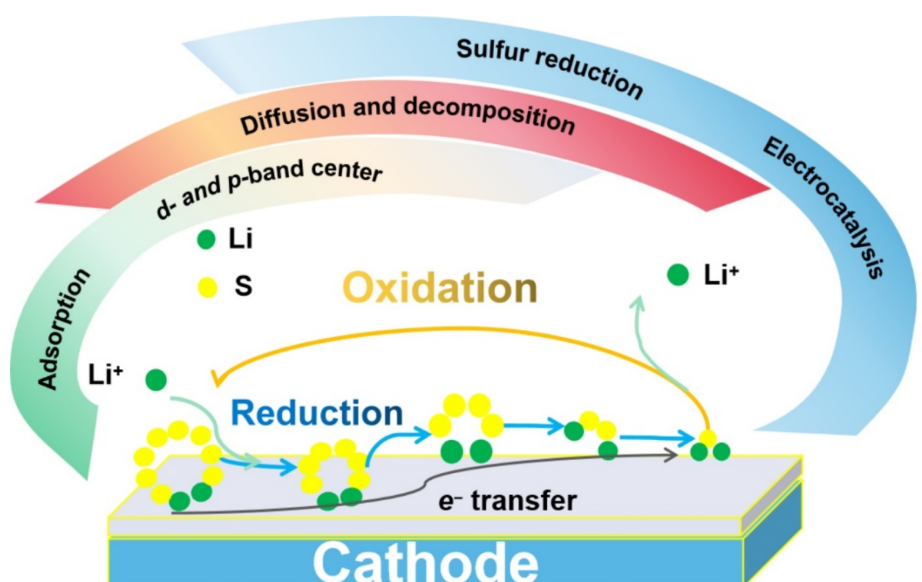
Although great progress has been achieved in Li–S batteries during past years, a deep insight into the working mechanism and rational design strategies of sulfur hosts is very lacking.<sup>60–66</sup> Beyond conventional experiments, theoretical simulations have been spread to chemistry, materials science, and energy fields.<sup>67–75</sup> Especially, density functional theoretical (DFT) calculations have been widely applied in Li–S batteries, such as probing the

adsorption of polysulfides on host materials.<sup>76,77</sup> Additionally, the lithium-ion diffusion barrier and Li<sub>2</sub>S decomposition barrier have been proposed to assess the polysulfides diffusivity and the delithiation kinetics on host materials, respectively.<sup>51,78</sup> Besides, the Gibbs free energy change during the conversion from sulfur to Li<sub>2</sub>S is another important criteria for evaluating the catalytic performance of cathode hosts.<sup>57</sup>

Nowadays, theoretical models play an increasingly important role in Li–S systems from probing the conversion reaction mechanism to designing sulfur host materials. In this review, we focus on the theoretical models for sulfur cathodes from model fundamentals to model applications (Scheme 1). The principle of theoretical models and the application in mechanistic understanding of the LiPSs adsorption and corresponding catalytic conversion are elaborately illuminated. Additionally, the relationships between the d-band center and the catalytic and adsorption performances of sulfur host materials are assessed by d–p band center models. Finally, future application of theoretical models in S cathode materials is provided.

## 2 | THEORETICAL MODELS FOR SULFUR CATHODE CONVERSIONS

Although Li–S batteries have attracted wide attention, the practical progress is impeded by a series of intractable problems deriving from sulfur cathodes.<sup>79</sup> Inhibiting the “shuttle effect” is a priority for improving the Li–S



**SCHEME 1** Schematic diagram of theoretical models, which assist the mechanism investigation and materials design of sulfur host for Li–S batteries

battery performance. Especially, the increase of sulfur loading, the decrease of electrolyte/sulfur ratio, the sluggish kinetics of LiPSs conversion, and the “shuttle effect” become obvious because of the accumulation of LiPSs on substracts.<sup>80,81</sup> Great efforts have been devoted to improving the reaction kinetics and S utilization by designing various sulfur hosts.<sup>21</sup> Simultaneously, the focus of sulfur hosts has experienced the transformation from LiPSs adsorption and Li<sup>+</sup> diffusion to LiPSs conversion.

DFT calculations are valid tools especially in understanding the polysulfides conversion mechanism in Li–S batteries. The development of theoretical models also underwent three stages: adsorption–diffusion–conversion. The investigations not only identify the performance of electrocatalysts but also explore the fundamental electrocatalytic mechanism of redox reaction in Li–S batteries.<sup>82–84</sup> According to the evolution of host descriptors based on DFT calculations, the existing theoretical models can be mainly divided into five kinds: adsorption model and lithium bond, lithium-ion diffusion and Li<sub>2</sub>S decomposition model, free energy model, *d*–*p* band center model, and SRR catalytic model. In the following sections, each model is discussed respectively.

## 2.1 | Adsorption model and lithium bond chemistry

The interaction strength, namely binding energy, between LiPSs and sulfur hosts is an extremely important parameter for resisting shuttle effects. Large binding energy is beneficial to both anchor LiPSs in cathodes and impede their shuttle process. Static adsorption of LiPSs is often conducted in experiments to test the anchoring ability of host materials. However, the experimental approaches are facing grand challenges to give a quantitative comparison between different host materials. On the contrary, adsorption models based on DFT calculations show great advantages. Not only the binding energy but also comprehensive geometrical and electronic structure analyses can be obtained. Generally, the binding energy between LiPSs and sulfur hosts is defined as follows:

$$E_{\text{ads}} = E(\text{total}) - E(\text{molecule}) - E(\text{host}), \quad (1)$$

where *E*(host), *E*(molecule), and *E*(total) represent the total energies of a host material, Li<sub>2</sub>S<sub>x</sub> (*x* = 1–8) or S<sub>8</sub> molecules, and the host adsorbed with one corresponding Li<sub>2</sub>S<sub>x</sub> or S<sub>8</sub> molecule, respectively.

Because of the distinguished electrical conductivity, high specific surface area, and lightweight, carbon materials have been widely investigated as sulfur hosts in both experiments and DFT calculations.<sup>77,85–89</sup> Specifically, the

adsorption of LiPSs on graphene, graphite, graphyne, carbon nanotube (CNT), C<sub>60</sub>, has been comprehensively studied.<sup>90–92</sup> These pure carbon materials usually deliver a weak interaction toward LiPSs, in which the physical interaction dominates. In order to enhance the interaction between LiPSs and carbon materials, heteroatom doping is particularly considered. The heteroatom such as nitrogen with lone pair electrons is supposed to form a strong Lewis acid–base interaction with the Li atom in LiPSs. Such Lewis acid–base interaction can be explained by the Li bond chemistry that LiPSs and heteroatom sites play as the Li donor and acceptor, respectively (Figure 1A).<sup>88,94</sup> Inspired by hydrogen bonds, Zhang and coauthors comprehensively study the geometrical structure, electronic structure, charge transfer, <sup>7</sup>Li chemical shift, and dipole moment of Li bonds.<sup>88</sup> Despite a small charge transfer, a large dipole moment was observed during the formation of Li bonds, which explains the origin of their large binding energy and further highlights their important role in sulfur host design. Accordingly, the chemical nature of Li bonds was determined as a dipole–dipole interaction for the first time, which paves the way for a rational and delicate design of Li bonds and corresponding sulfur host materials. Especially, the <sup>7</sup>Li nuclear magnetic resonance connects the experimental and theoretical design of Li bonds as a strongly Li bond can induce an obvious upshift to the low field in <sup>7</sup>Li NMR spectra (Figure 1B,C).

Beyond nitrogen doping, other heteroatom doping such as boron, oxygen, fluorine, phosphorus, and sulfur are systematically studied by Hou et al. (Figure 1D).<sup>93</sup> The adsorption capacities of heteroatom-doped graphene nanoribbons (GNRs) toward LiPSs are sensitive to dopant elements by analyzing binding energy, geometrical configuration, and electronic structures. N and O dopants provide more adequate interactions to LiPSs than other doped elements. This strong interaction with LiPSs is associated with the radii, electronegativity, polarity, and dipole moments of heteroatoms. General principles of designing heteroatom-adopted carbon as sulfur hosts were further proposed and summarized as follows (Figure 1E).<sup>93</sup>

1. A lone pair of electrons is necessary for doping atoms;
2. The electronegativity and the radius of the doping atom emerge as the screening indicators for heteroatom-doped GNRs;
3. The strength of dipole–dipole interaction is the pivotal descriptor for heterogeneous surface interaction;
4. Stable bonding between the doping atom and the carbon plane could restrain the reaction between the host and LiPSs.

Furthermore, an implicit volcano curve expounds the underlying dependence of binding energies on the

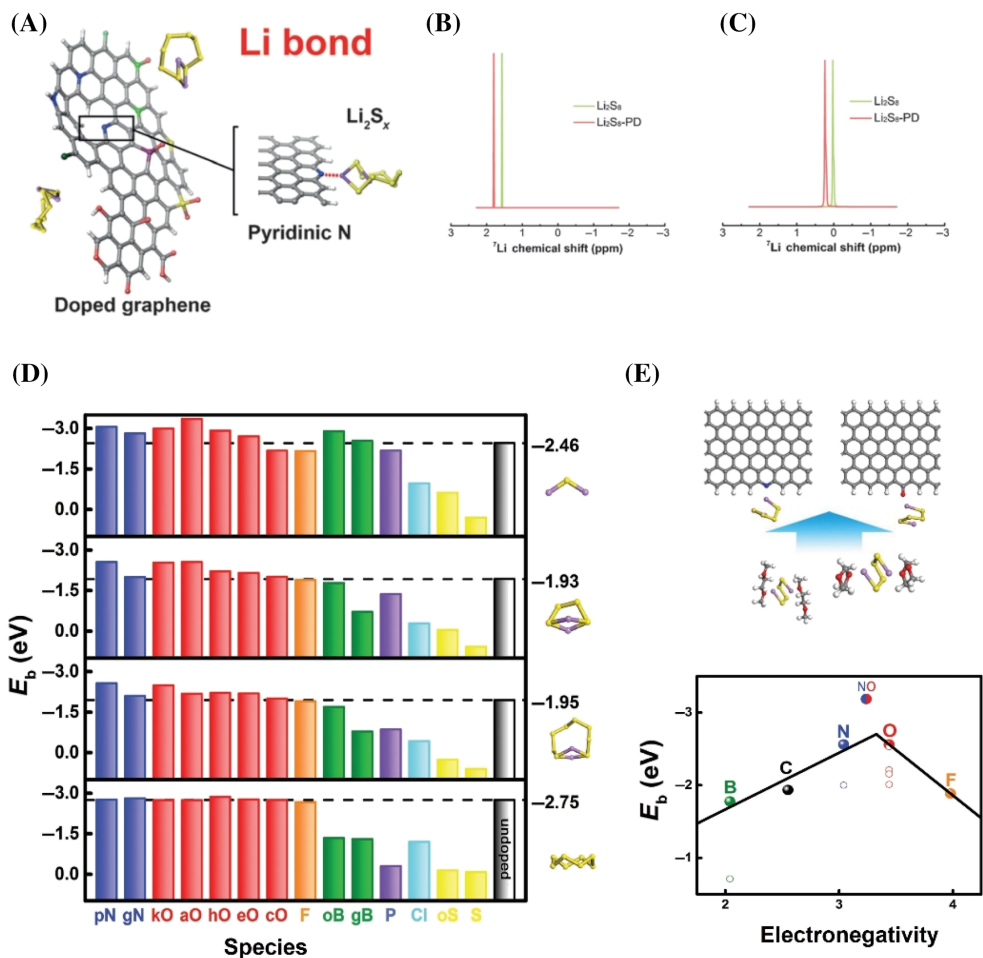


**FIGURE 1** Li bonds chemistry and polysulfide adsorption on pristine or heteroatom-doped graphene. (A) Li bonds in Li-S batteries. The identification of Li bonds with (B) theoretical and (C) experimental NMR characterizations. Reproduced with permission of reference 88. Copyright 2017. Wiley-VCH. (D) The binding energies of undoped and heteroatom-doped GNRs. (E) The volcano plot of  $\text{Li}_2\text{S}_4$  binding energy against the electronegativity of heteroatoms. Reproduced with permission of reference 93. Copyright 2016. Wiley-VCH

electronegativity of dopants and delivers fancy strategies for a rational design of Li bonds (Figure 1E). The dipole-dipole interaction strengthens with the increase of electronegativity of dopants due to the growing negative charge on doped atom in carbon lattice. Since N and O atoms are adjacent to the top of volcano, (N, O) codoped GNR was built to break the rule of monodoped GNRs. The synergies between nitrogen and oxygen in GNR facilitate strong dipoles and further offer preferable affinity and strong anchoring sites to LiPSs. These analyses and prediction have been validated by amounts of efforts<sup>95,96</sup> and deepen the understanding of the adsorption properties.

Beyond heteroatom-adopting, polar materials are also widely introduced into composite carbon cathodes to immobilize LiPSs and thereby impede shuttle effects. For example, well-dispersed  $\text{Nb}_2\text{O}_5$  nanocrystals in mesoporous carbon microspheres,<sup>97</sup>  $\text{Fe}_3\text{C}$  embedded in porous carbon sheets (i.e.,  $\text{Fe}_3\text{C}@\text{NPCS}$ ),<sup>98</sup> dispersed

VN nanoparticle into N-doped graphene (VN/N-rGO),<sup>99</sup> and MoN-C-MoN trilayer architecture as two-sided nitride surfaces (Figure 2).<sup>100</sup> Regulating the interaction between LiPSs and the polar materials is the key for these composite cathode hosts.

However, the adsorption on polar materials is much more complicated than that on graphene. Different polar materials can deliver varied binding energy trends of LiPSs. Even for a specific polar material, the selection of exposed crystal plane and exposed terminal atoms has a significant influence on the adsorption of LiPSs. Besides, chemical interaction is usually dominated in the adsorption of LiPSs on polar materials.

To differ the chemical and physical interactions, the ratio for van der Walls (vdW) interaction is proposed to uncover the anchoring mechanism for various anchoring materials (AMs) during different lithiation stages (Figure 3A,B).<sup>101</sup> The ratio for vdW interaction is defined as follows:

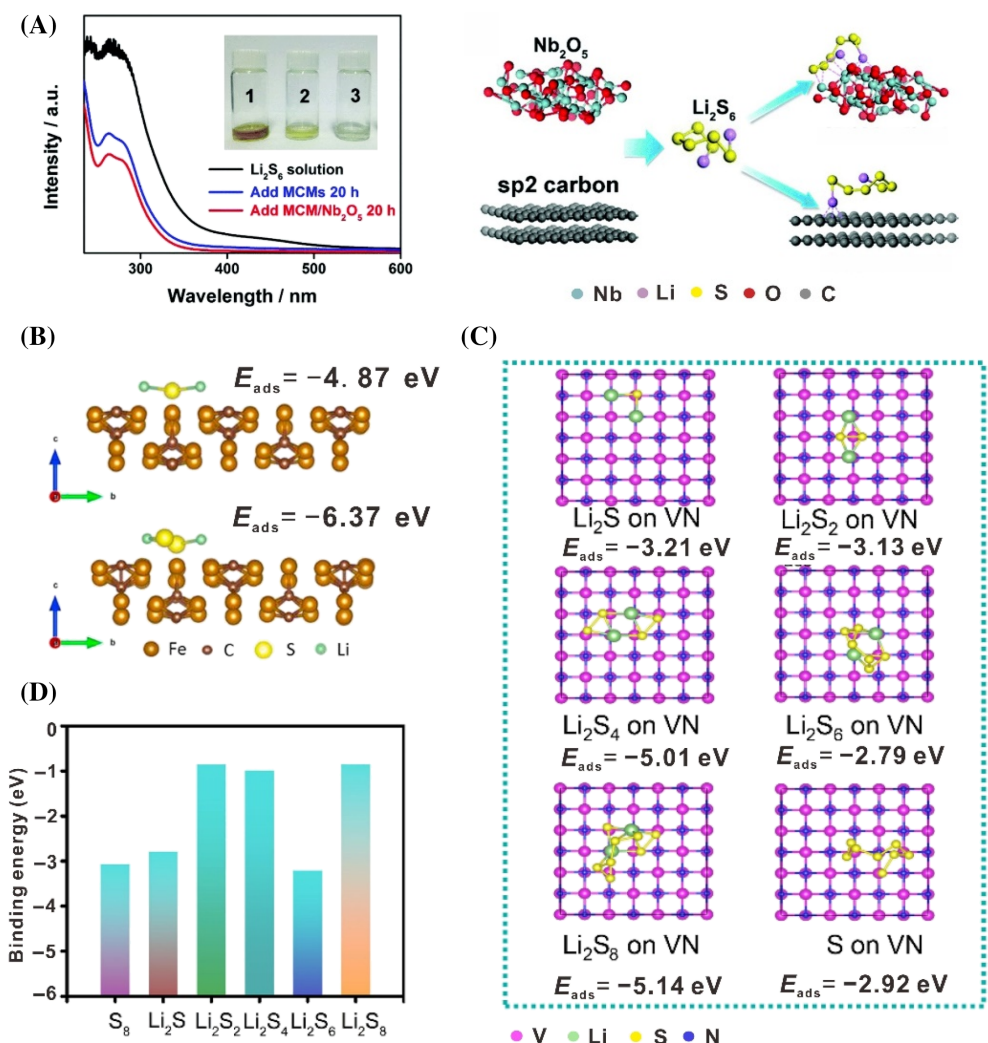


**FIGURE 2** Studies for kinetic improvement of polysulfide redox reactions by polar materials. (A) UV/vis absorption spectra and binding geometric configurations of LiPSs with Nb<sub>2</sub>O<sub>5</sub> nanocrystals. Reproduced with permission of reference 97. Copyright 2016. The Royal Society of Chemistry. (B) Optimized adsorption configuration of Li<sub>2</sub>S and Li<sub>2</sub>S<sub>2</sub> on the Fe<sub>3</sub>C surface. Reproduced with permission of reference 98. Copyright 2019. Elsevier. (C, D) Modulation of the polysulfides transformation by vanadium nitride nanoparticle/3D porous graphene: the adsorption configurations and binding energies of Li<sub>2</sub>S<sub>x</sub> species on VN(001) surface. Reproduced with permission of reference 99. Copyright 2020. Elsevier

$$R = \frac{(E_b^{\text{vdW}} - E_b^{\text{no vdW}})}{E_b^{\text{vdW}}}, \quad (2)$$

where  $E_b^{\text{vdW}}$  and  $E_b^{\text{no vdW}}$  represent the binding energy with and without vdW interaction, respectively. Accordingly, the materials can be categorized into strong, moderate, and weak AMs by the vdW interaction ratio. Specifically, the vdW interaction ratio of strong AMs like oxides is low, in which the chemical interaction dominates (Figure 3A). On the contrary, physical interaction dominated AMs like chlorides have a large vdW interaction ratio. Impressively, the optimal choices for S cathode are moderate sulfides materials that possess two dominated interactions during different lithiation stages

(physical interaction for under lithiation stage and chemical interaction after that). These interactions induce moderate binding strength and retain LiPSs configurations from dissolving into the electrolyte.

A deep analysis of the electronic structure of sulfur hosts is very powerful to reveal the interaction mechanism and explain varied binding energies for different AMs. For example, a strong interaction often delivers an obvious charge transfer, which can be revealed by differential charge or Bader charge analyses. Different from weak physical adsorption, a significant charge transfer between Li atoms in polysulfides and O or S atoms in metallic compounds is often accompanied by strong chemical adsorption (Figure 3C). The atomic partial density of states (PDOS) further illustrates the underlying

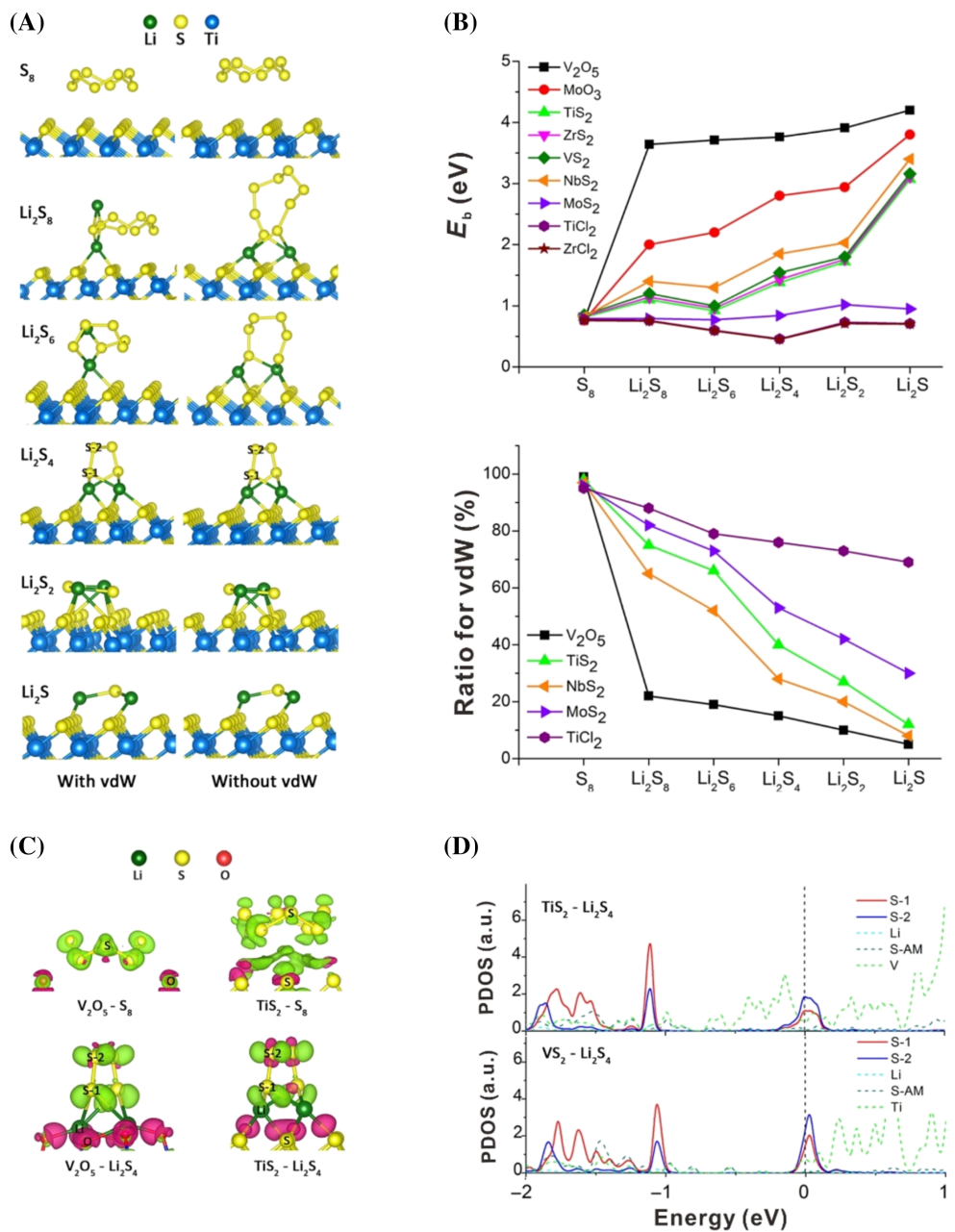


**FIGURE 3** The anchoring mechanism for various AMs. Interaction mechanism between AMs and LiPSs assessed by the ratio for vdW interaction (A) Li-S composites on TiS<sub>2</sub> configurations; (B) the binding energies and ratio for vdW interaction for polysulfides on different nanoscale anchoring materials; (C) charge transfers and (D) atomic partial density of state near Fermi energy region for polysulfides and metal-based materials. Reproduced with permission of reference 101. Copyright 2015. American Chemical Society

determinant for the binding strengths, that is, the location of Fermi energy for various metal-based materials (Figure 3D).

The analysis of electronic structures can also reveal the origin of varied binding energies of LiPSs on different AMs. Zhang and coworkers explored the intrinsic differences among analogous AMs by DFT calculations.<sup>102</sup> S-binding is dominated binding configurations for LiPSs adsorption on transition metal sulfide (TMS) cathodes, originating from the charge transfer between

metal atoms in TMS and S atoms in LiPSs (Figure 4A). According to further PDOS analysis (Figure 4B,C), the charge transfer is mainly attributed to the *d-p* orbital interaction between TMS and LiPSs. Consequently, the binding energy is featured by the amount of *d*-electrons of the metal. A periodic volcano plot describes the relationship between the binding energy and the *d*-electron numbers (Figure 4D), which provides simple and general guidelines for designing and screening host materials.

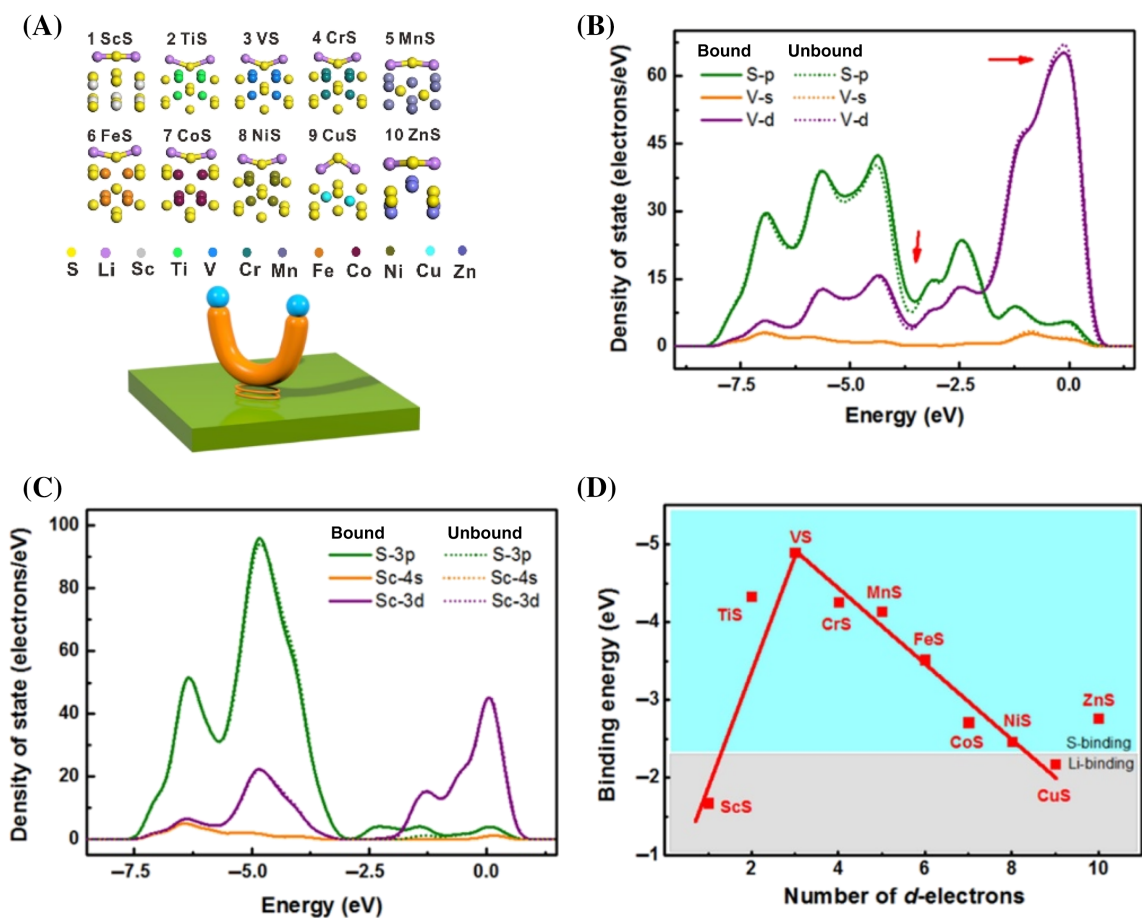


**FIGURE 4** The intrinsic differences among analogous metal sulfides. (A)  $\text{Li}_2\text{S}$  adsorbed configurations and schematic of the metal–sulfur bond; (B) periodic trend of binding energies between metal sulfides and  $\text{Li}_2\text{S}$ . (C) Relationship of charge transfer versus binding energy and (D, E) PDOS for the transition metal sulfide adsorption systems. Reproduced with permission of reference 102. Copyright 2017. American Chemical Society

In short, the adsorption model and lithium bond could evaluate the anchoring effect on host–guest interface in Li–S batteries. In-depth analysis of electronic structures not only clears the intrinsic differences of host materials but also distinguishes the unique interaction between LiPSs and different host materials. These conclusions provide theoretical supports and rules to guide the future screening and design of host materials.

## 2.2 | Lithium-ion diffusion and $\text{Li}_2\text{S}$ decomposition models

Although polar materials could facilitate the capture of LiPSs, most of them are insulators, resulting in the accumulation of LiPSs in electronically inactive areas. The diffusion of  $\text{Li}_2\text{S}_x$  species on solid substrates is an important factor for Li–S battery electrochemical performance. A rapid diffusion contributes to the LiPSs electrochemical reaction and  $\text{Li}_2\text{S}$  uniform growth on the sulfur cathode.

However,  $\text{Li}_2\text{S}_x$  species diffusion has always been contrary to the adsorption of polysulfide on solid substrates. How to balance the adsorption and diffusion of LiPSs on the surface is complicated. A diffusion model can help to solve these complex issues.

Since Li atoms in  $\text{Li}_2\text{S}_x$  are the favorable binding site with substrates, Cui and coworkers developed a model for the diffusion of lithium across various metal compounds instead of the diffusion of sulfide species (Figure 5A,B).<sup>51,78</sup> They designed diverse pathways to transport Li ions along with various directions. The diffusion barriers for Li ion along the diffusion pathway are subsequently calculated by climbing image nudged elastic band (CI-NEB) methods. The diffusion barrier reflects the diffusion kinetics of LiPSs. The trend of diffusion rate is going in the opposite direction with the height of the diffusion barrier (Figure 5A). A small diffusion barrier reveals an enhanced diffusion rate.  $\text{MgO}(100)$  delivers the lowest diffusion barrier among investigated metal oxides, which explains the excellent cycling performance

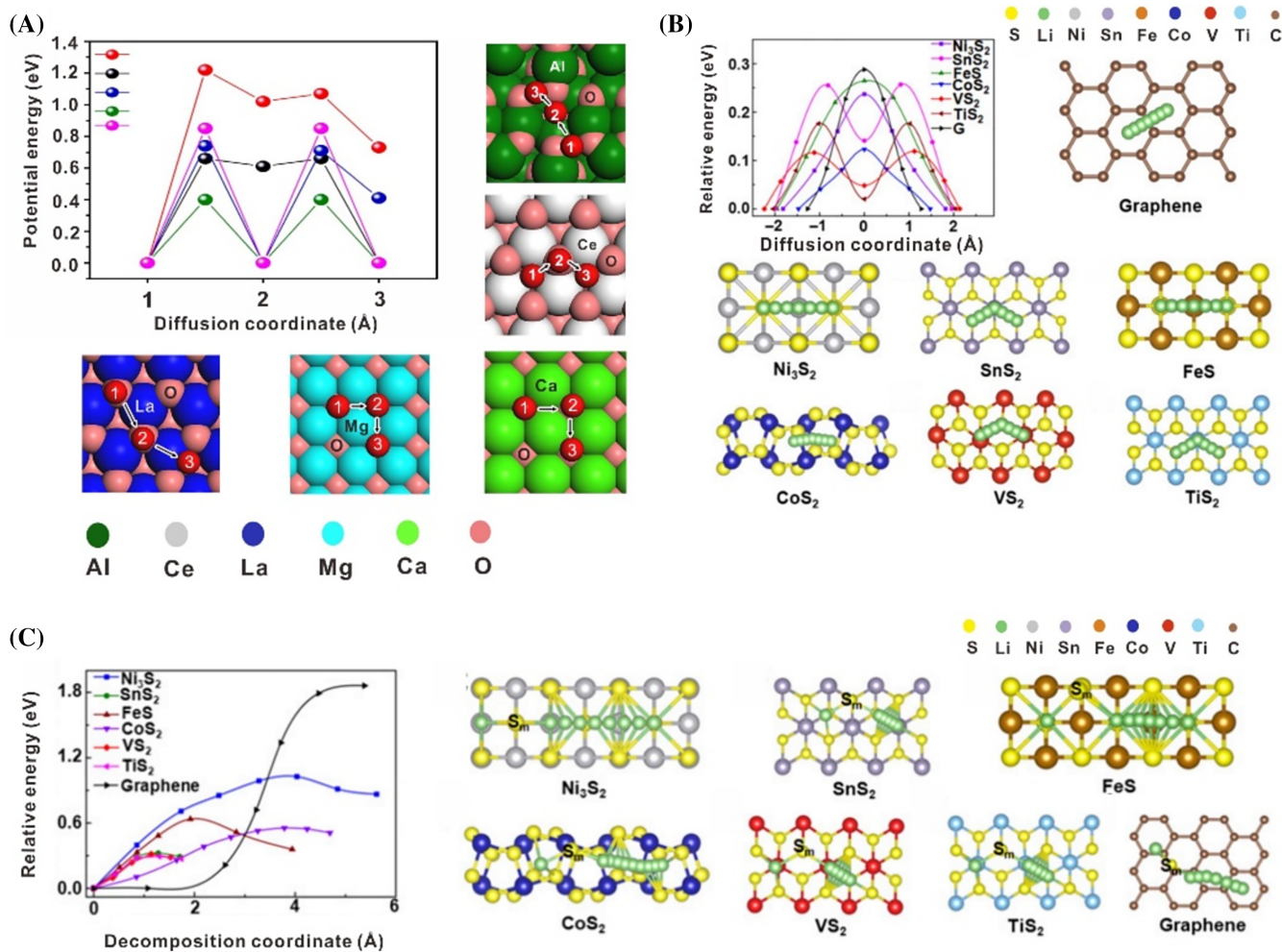
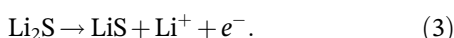


**FIGURE 5** Lithium-ion diffusion and Li<sub>2</sub>S decomposition mechanisms. (A) Along with different adsorption sites on the oxide surface; Reproduced with permission of reference 51. Copyright 2016. Springer. (B) The surface of various metal sulfides and graphene. (C) Li<sub>2</sub>S decomposition mechanism on the surface of various metal sulfides and graphene. Reproduced with permission of reference 78. Copyright 2017. National Academy of Sciences

of MgO/C cathodes. The model for the Li ion diffusion was applied on metal sulfides and the results are also consistent with the experimental observations (Figure 5B).<sup>78</sup> These calculations elucidate the origin and rationality of using the lithium-ion diffusion barrier as a descriptor for reaction kinetics on various electrodes.

Furthermore, the catalytic oxidation of Li<sub>2</sub>S is crucial for achieving high reversible capacity and long cycling life during battery charging because of two pathways in which Li<sub>2</sub>S is formed, namely electrochemical deposition and chemical disproportionation. The host materials should have the catalytic capability to facilitate Li<sub>2</sub>S oxidation. Therefore, Cui and coworkers developed a Li<sub>2</sub>S decomposition model to demonstrate the oxidation of Li<sub>2</sub>S on various materials. It was assumed that one Li atom is far away from Li<sub>2</sub>S during the decomposition of Li<sub>2</sub>S. Li<sub>2</sub>S is divided into a LiS cluster and a single Li ion as followed:



Then, the barrier for the delithiation process was simulated by CI-NEB methods. The calculated decomposition barrier corresponds to the measured voltage magnitudes experimentally, which could reflect the catalytic Li<sub>2</sub>S oxidation kinetics on different hosts. As seen from the pathway plots (Figure 5C), low activation energy leads to improved capacity and cycling stability of Li-S batteries. Besides, the size of the decomposition barrier depends on the chemical interaction between Li ions and the host materials. The binding ability of hosts for LiPs governs the Li<sub>2</sub>S decomposition and overall performance of Li-S batteries. Therefore, the Li<sub>2</sub>S decomposition model not only uncovers the oxidizing capability of host materials but also demonstrates the reason for different oxidation kinetics of Li<sub>2</sub>S, which provides a theoretical basis for further development of electrode materials in catalyzing the oxidation of Li<sub>2</sub>S back to sulfur.

Based on these models, Zhao and coauthors predicted that two-dimensional magnetic  $\text{Fe}_3\text{GeX}_2$  ( $\text{X} = \text{S}, \text{Se}$ , and  $\text{Te}$ ) monolayers could be potential candidates which possess bifunctional electrocatalytic activity to the SRR and the  $\text{Li}_2\text{S}$  decomposition reaction.<sup>103</sup> Zhang

and coauthors explored the possibility of  $\alpha$ -tellurene as the host material in Li-S batteries.<sup>104</sup> Xiong's group proposed a novel kind of tungsten (W) single atomic catalyst with high LiPSs adsorption ability and catalytic activity (Figure 6).<sup>105</sup>

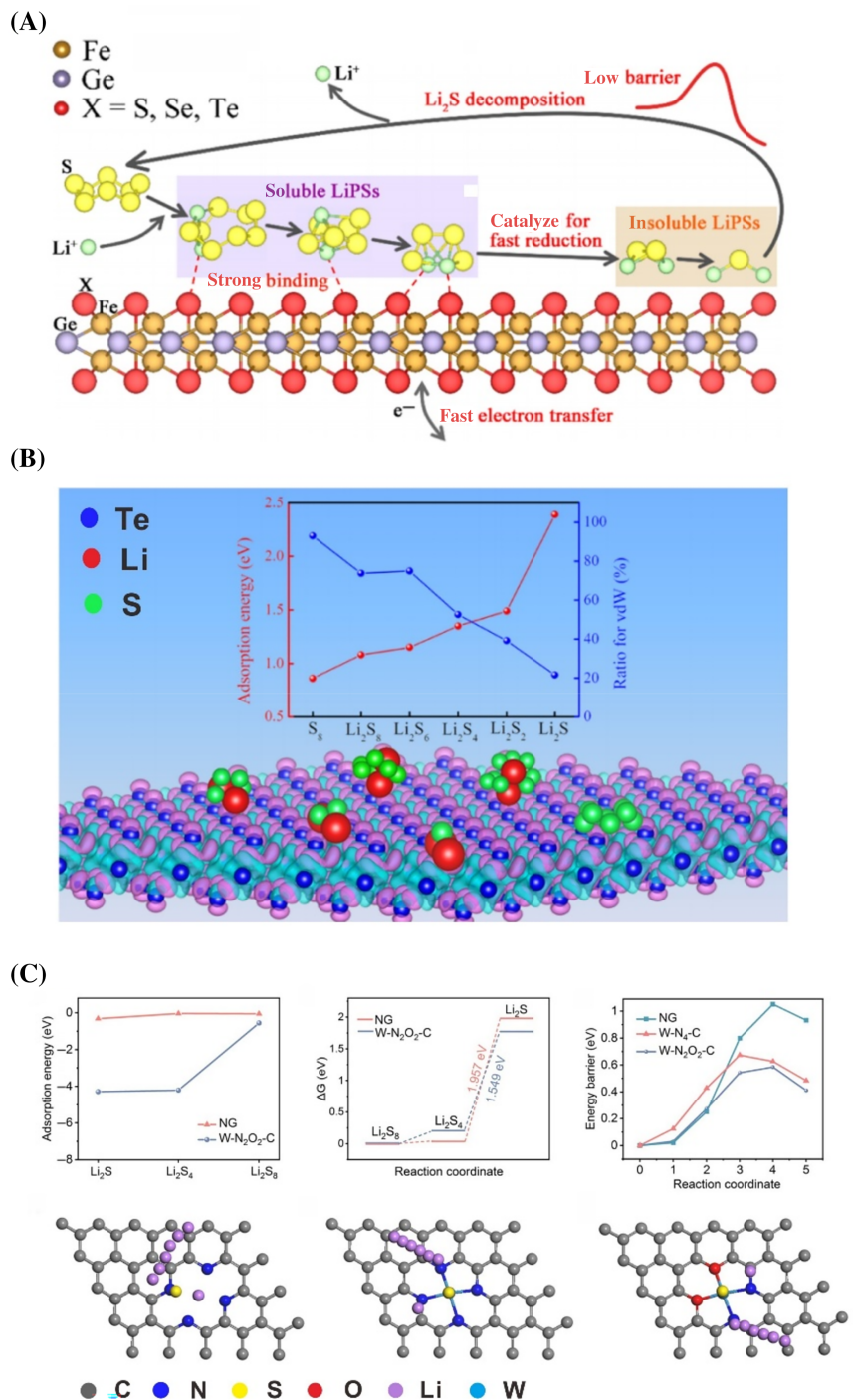


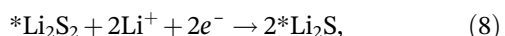
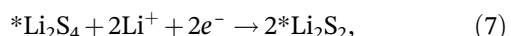
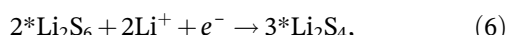
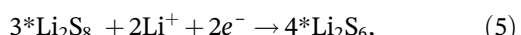
**FIGURE 6** The application of Lithium-ion diffusion and  $\text{Li}_2\text{S}$  decomposition models. (A) The reaction process of sulfur on  $\text{Fe}_3\text{GeX}_2$  monolayers. Reproduced with permission of reference 103. Copyright 2021. American Chemical Society. (B) Predicting the possibility of  $\alpha$ -tellurene as the host material in Li-S batteries. Reproduced with permission of reference 104. Copyright 2021. American Chemical Society. (C) A novel kind of tungsten (W) single atomic catalyst immobilized on nitrogen-doped graphene (W/NG) as a highly active multifunctional catalytic site. Reproduced with permission of reference 105. Copyright 2021. Wiley-VCH

### 2.3 | SRR model

The SRR is a complex 16-electron conversion process. Nevertheless, the sluggish liquid–solid transformation of SRR reduces the rate capability and cycle life of Li–S batteries. Following the pioneering work of Nazar and coworkers,<sup>106</sup> electrocatalysts were proposed as effective strategies to address the slow kinetics of the LiPSs redox reaction.<sup>107–109</sup>

A deep understanding of the electrocatalytic SRR mechanism is beneficial to the rational design of high-performance electrocatalysts.

Currently, the LiPSs conversion on the electrocatalysts has been investigated by simulating the reduction reaction from  $S_8$  to  $Li_2S$ . Kong and coworkers calculated the Gibbs free energies of each S reduction pathway to assess the catalytic properties of host materials.<sup>57</sup> The reaction of sulfur reduction is considered as follows:<sup>110,111</sup>



where  $*$  is the catalyst. Then they calculated the Gibbs free energies of each path for the above reactions. The equations of these variations of Gibbs free energies are written as follows:

$$\Delta G_1 = G({}^*Li_2S_8) - G({}^*S_8) - 2G(Li), \quad (9)$$

$$\Delta G_2 = 4G({}^*Li_2S_6) - 3G({}^*Li_2S_8) - 2G(Li), \quad (10)$$

$$\Delta G_3 = 3G({}^*Li_2S_4) - 2G({}^*Li_2S_6) - 2G(Li), \quad (11)$$

$$\Delta G_4 = 2G({}^*Li_2S_2) - G({}^*Li_2S_4) - 2G(Li), \quad (12)$$

$$\Delta G_5 = 2G({}^*Li_2S) - G({}^*Li_2S_2) - 2G(Li). \quad (13)$$

In Equations (4)–(8),  $G(Li^+) + G(e^-)$  are replaced by  $G(Li)$  and considered in the condition of 0 V versus Li/ $Li^+$  electrode, which is similar to the method of hydrogen electrode:

$$G(Li^+) + G(e^-) = G(Li) - eU. \quad (14)$$

The  $G(Li)$  represents the Gibbs free energy of Li solid and  $U$  is the potential versus Li/ $Li^+$  electrode. Finally, the rate-limiting step in the entire sulfur reduction

process is determined by the value of Gibbs free energy change.

The catalytic origin and properties with various electrocatalysts are further revealed by the calculated Gibbs free energy changes. Figure 7A shows the free energy profiles of two substrates (cobalt atom embedded in nitrogen-doped graphene (Co–N/G) and nitrogen-doped graphene (N/G)). By comparing the Gibbs free energy of each step, the formation of  $Li_2S$  from  $Li_2S_2$  is the rate-limiting step. While a low value of Gibbs free energy change for the rate-limiting step is thermodynamically favorable for S reaction on electrocatalyst. Based on this model, Kong et al. revealed the reason why Co–N/G has excellent electrochemical performance.<sup>57</sup> Chen and coworkers used a similar approach to uncover the improved catalytic activity of  $MoS_2$  toward LiPSs (Figure 7B).<sup>112</sup> Similar conclusions were made: (1) The more negative exothermic step, the faster kinetics of LiPSs reduction path than those endothermic or nearly thermoneutral paths. (2) The reduction of  $Li_2S_2$  to solid-state  $Li_2S$  is the rate-limiting step. (3) Minor changes in Gibbs free energy of the rate-limiting step empowered  $MoS_2$  to promote the catalytic effect on soluble LiPSs and inhibit the shuttle effect in the discharge process.

It is advantageous for screening rational electrocatalysts and studying the intrinsic mechanism by

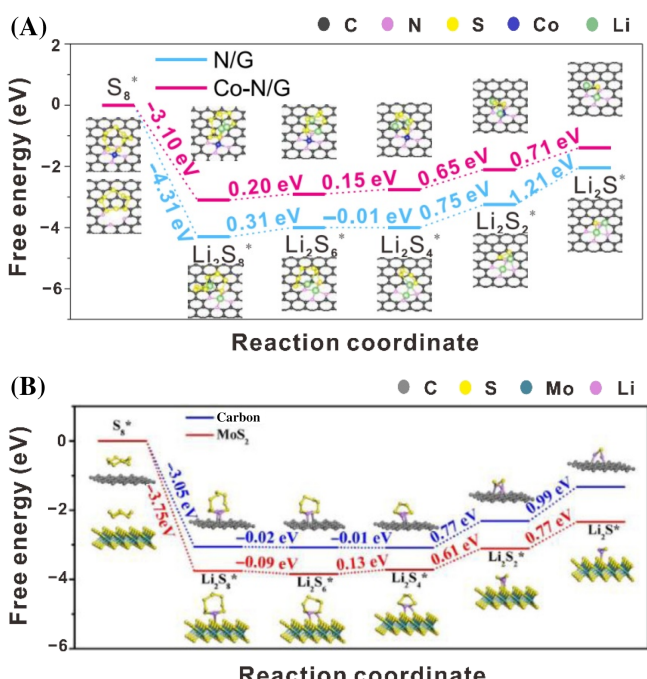


**FIGURE 7** Free energy profiles for the reduction of LiPSs on different substrates. (A) N/G and Co–N/G substrates. Reproduced with permission of reference 57. Copyright 2019. American Chemical Society. (B) Carbon and  $MoS_2$  substrates. Reproduced with permission of reference 112. Copyright 2020. Elsevier

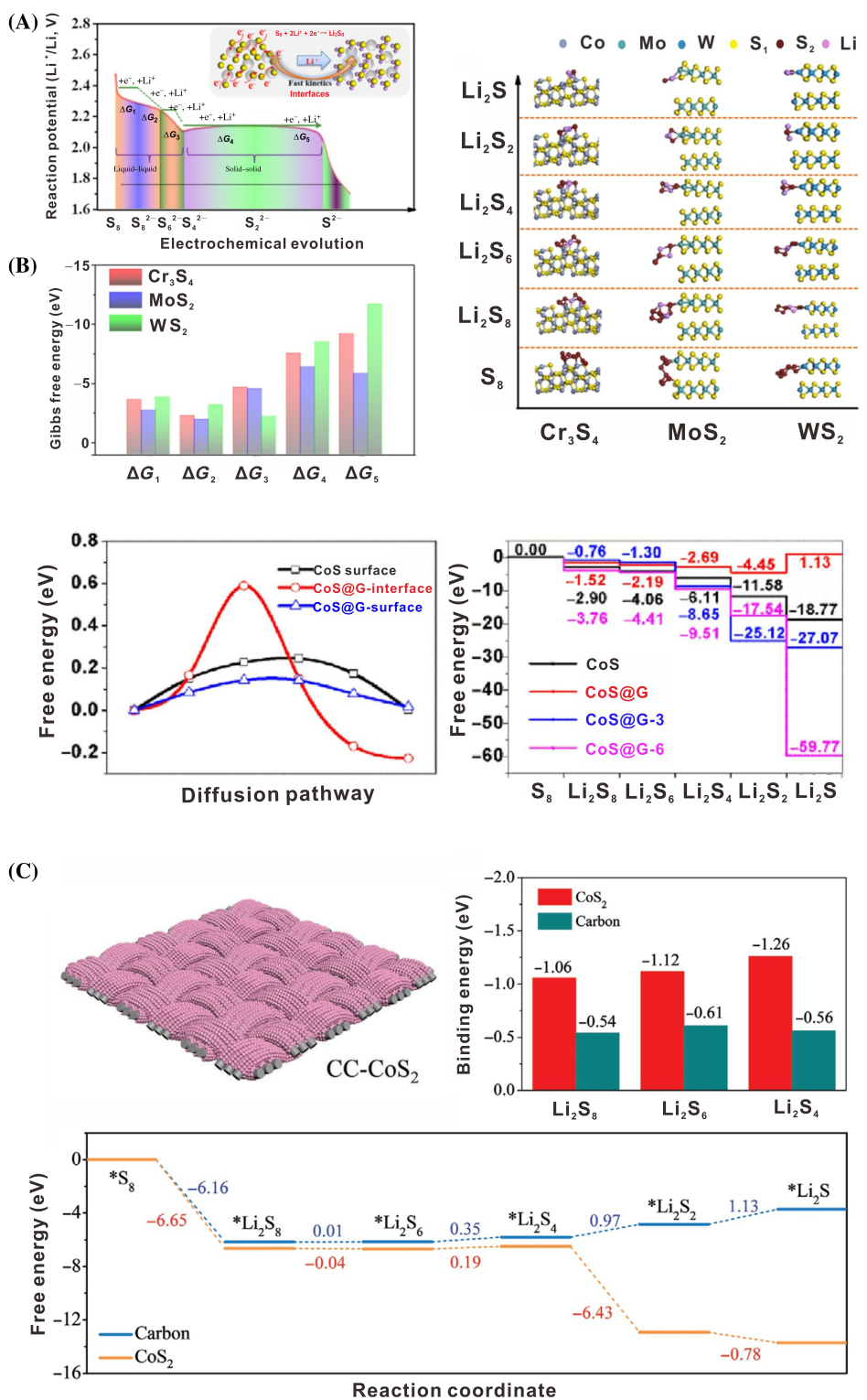


**FIGURE 8** Comprehensive application of theoretical models. (A) Investigation of the effect of metal sulfides  $\text{M}_x\text{S}_y$  ( $\text{M} = \text{Cr}, \text{Mo}$ , and  $\text{W}$ ) in the conversion of polysulfides. Reproduced with permission of reference 114. Copyright 2020. American Chemical Society. (B) Investigation of the exposed interfaces of CoS at the defective sites of the graphene coating as anchoring materials. Reproduced with permission of reference 115. Copyright 2021. Elsevier. (C) CoS<sub>2</sub>-modified carbon clothes as sandwiched cathodes for Li-S batteries. Reproduced with permission of reference 116. Copyright 2021. Wiley-VCH

integrating these theoretical models in Li-S batteries.<sup>113</sup> For instance, Wang, Li, Zhang, and coworkers investigated the lithiation processes from  $\text{S}_8$  to  $\text{Li}_2\text{S}$  on

two-dimensional metal sulfides ( $\text{M}_x\text{S}_y$ ,  $\text{M} = \text{Cr}, \text{Mo}$ , and  $\text{W}$ , which have half-filled  $d$  orbitals) to understand the performance diversity of various electrocatalysts.<sup>114</sup>

The lithiation processes on different materials were presented by the adsorption model as displayed in Figure 8A. Each lithiation reaction occurs on the surface of the electrocatalysts, thus the difference of the electron densities of surfaces has a significant influence on the Gibbs free energy changes. The reasonable catalyst can be used to regulate the Gibbs free energy changes of LiPSs conversions thermodynamically, and thereby Cr<sub>3</sub>S<sub>4</sub>/C and WS<sub>2</sub>/C cathodes are chosen as ideal anchoring materials. Additionally, He, Li, and coworkers optimized the performance of Li-S batteries by constructing a sandwich-structured interlayer,<sup>115</sup> which also possesses strong adsorption and high catalytic capability for LiPSs simultaneously.<sup>117</sup> The functional interlayer consists of CoS nanosheets and a reduced graphene oxide coating (RG) based on carbon nanofiber membranes.<sup>115</sup> The high catalytic activity of functional interlayer is due to its unique 3D construction inducing a synergistic catalytic effect, the low barrier of Li<sup>+</sup> diffusion on graphene surface, and strong adsorption energy for the transformation of LiPSs on CoS interface (Figure 8B). The functional interlayer not only decreases the Li<sub>2</sub>S decomposition barrier but also regulates the LiPSs formation efficiently. Considering the favorable catalytic properties of CoS<sub>2</sub>, a sandwiched cathode composed of carbon clothes modified by CoS<sub>2</sub> was designed.<sup>116</sup> It confirms from theoretical simulations that large negative Gibbs free energy on the surface of cathodes is responsible for the high catalytic activity (Figure 8C). Su et al. also employed theoretical models to explain the improved reaction thermodynamics by the Fe<sub>3</sub>O<sub>4</sub>/CNSs-PP separator as well.<sup>118</sup> Consequently, the combination of these theoretical models contributes not only to seeking out electrocatalysts but also to a deep understanding of the mechanism of sulfur cathodes electrocatalysis.

## 2.4 | *d*- and *p*-band center models

As discussed above, moderate surface adsorption and charge transfer are beneficial to facilitate the electrochemical conversion in sulfur cathodes. However, the interfacial interaction is essentially associated with the surface electronic structure of the adsorbed substrates. It is necessary to understand the inherent modulating mechanism of the interfacial interaction, especially at the electronic structure levels.

Recently, the *d*- and *p*-band center models could unlock the underlying mechanism for different performances (adsorption energy and catalytic energy barrier) in various anchoring materials. For example, Qian's group mainly explored the effects of the *p* orbitals of

non-metal anions on regulating the performance of Li-S battery. They proposed a *p*-band center model according to the kinetic behavior of LiPSs on a series of Co-based compounds, whose anions are alterable (Figure 9A).<sup>119</sup> Symmetrical electrochemical studies show that the kinetics for LiPSs conversion reaction are different on various Co-based compounds due to the *p* bands shift along with the change of anions. CoP presents the excellent rate performance and power density among the Co-based compounds since the *p*-band center of P moves toward the Fermi level, resulting in a narrow gap between Co 3d and P 2p band centers. A shrinking energy gap between the bonding and antibonding orbitals could accelerate the electron transfer and then the conversion of LiPSs, which is responsible for the high performance of CoP-based sulfur cathodes. The *p*-band center model reveals the contribution of *p* orbitals of the anions on electrochemical properties and offers a new insight to deciphering the modulating essence of the various metal-based compounds. In addition, the source of different electrochemical performances with various Fe-based sulfur hosts was also studied from both theoretical and experimental aspects.<sup>120</sup> Metal phosphide host in Li-S battery shows superior electrochemical performance by systematically comparing oxide- and phosphide-based sulfur hosts (CF/Fe<sub>3</sub>O<sub>4</sub>@C and CF/FeP@C). The conclusion is the same as Qian's work on the contribution of anions *p* orbitals for the Li-S system (Figure 9B). The *p*-band center in FeP shifts closer to the Fermi level than that in Fe<sub>3</sub>O<sub>4</sub>, which induces a narrowed gap between bonding and antibonding orbitals in FeP. The narrowed gap accelerates the combination and detachment of P atoms with or from other atoms, thus facilitating the electron transfer and LiPSs conversion. Analogously, Liu and coworkers utilized *d*-*p* band models to explain the electrochemical performance differences of Li-S batteries, whose separators are composed of a series of iron-based particles (Fe<sub>3</sub>O<sub>4</sub>@C, FeS@C, or Fe<sub>3</sub>N@C).<sup>122</sup>

Except for regulating the *p*-band center, the host materials could also be modified by adjusting the energy center of the *d* band relative to the Fermi level. According to *d*-band theory,<sup>123</sup> the shift of the *d*-band center of metal toward the Fermi level increases the probability of electrons filled in the antibonding orbital between metal and adsorbed molecules, which boosts the adsorption ability for sulfur species. Zhang and coworkers proposed a *d*-band tuning strategy through alloying cobalt to the metal sites of Ni<sub>2</sub>P.<sup>121</sup> Analyzing the simulation results, the *d*-band center of metal sites in Ni<sub>2</sub>Co<sub>4</sub>P<sub>3</sub> moves toward the Fermi level owing to the higher Co 3d band than Ni 3d band (Figure 9C), leading to a higher adsorbability and a lower activation barrier for Ni<sub>2</sub>Co<sub>4</sub>P<sub>3</sub> than that for

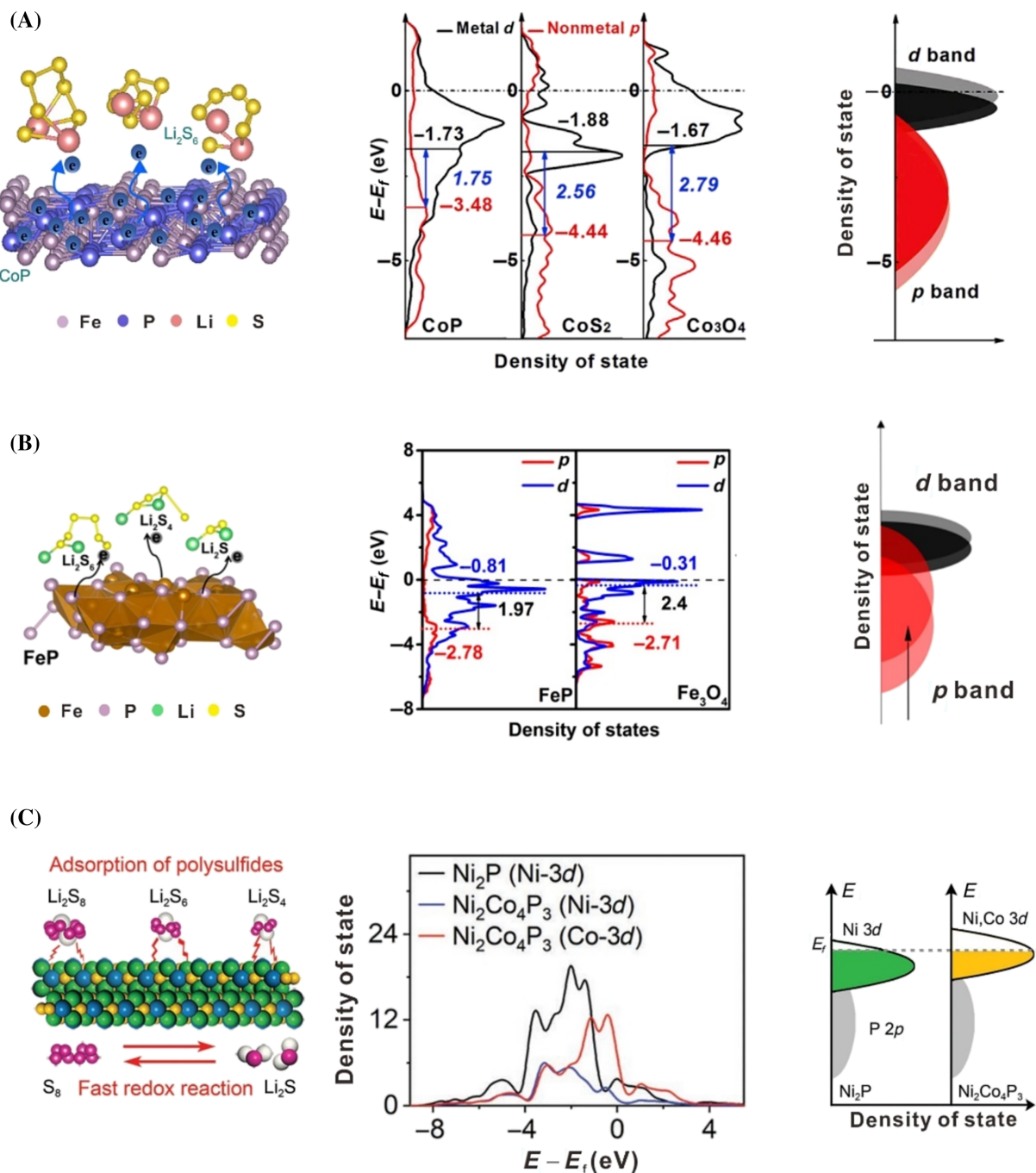


**FIGURE 9** Understanding the underlying mechanism with  $d$ - and  $p$ -band center models. The density of states analysis and band shifts of the  $p$  bands of anions and the  $d$  band of (A) Co in  $\text{CoP}$ ,  $\text{CoS}_2$ , and  $\text{Co}_3\text{O}_4$ , respectively; Reproduced with permission of reference 119. Copyright 2018. Elsevier. (B) Fe in  $\text{Fe}_3\text{O}_4$  and  $\text{FeP}$ . Reproduced with permission of reference 120. Copyright 2019. American Chemical Society. (C) The variation of density of states and  $d$ -band shift upon cation doping. Reproduced with permission of reference 121. Copyright 2020. Wiley-VCH

$\text{Ni}_2\text{P}$ . Additionally, Zhang, Chan, and coworkers fabricated an effective electrocatalyst ( $\text{Ni}_3\text{Fe}@\text{HPC-CNT}$ ) including an alloy of Ni and Fe inspired by the  $d$ -band model. Alloying metallic Ni with Fe modulates the  $d$ -band center of Ni and improves the corresponding absorption and catalytic capability for LiPSs, which further verifies the experimental results.<sup>80</sup>

Given the discussion above, the  $p$ - and  $d$ -band center models play an important role in explaining the adsorption capacity and catalytic ability in the conversion process of Li-S batteries. The position of band centers toward the Fermi level of non-metal anions/metal cations is responsible for the multifarious electrochemical performance of metal-based compounds in Li-S batteries.

## 2.5 | Electrocatalysis model

Although the aforementioned theoretical models could evaluate the catalytic performance of host materials at the molecular level, there is still a lot to be done in clarifying the origin of the SRR. Duan's group explored the electrocatalytic kinetics of the complicated SRR from an activation energies perspective (Figure 10A,B) and constructed a theoretical model to elucidate the origin of the electrocatalyst, that is, heteroatom-doped holey graphene framework (HGFs).<sup>82</sup>

On account of the large activation energy of  $\text{Li}_2\text{S}_2$  converted into insoluble  $\text{Li}_2\text{S}$ , the final two-electron reaction ( $\text{Li}_2\text{S}_2 + 2\text{Li}^+ + 2e^- \rightarrow 2\text{Li}_2\text{S}$ ) is focused on. Because

of the high correlation between the catalytic activity and the thermodynamic overpotential ( $\eta$ ) for the final two-electron reaction, the thermodynamic overpotential as a function of the adsorption Gibbs free energy of a LiS radical intermediate ( $\Delta G[\text{LiS}\cdot^*]$ ) is established to estimate the properties of catalysts.

First, it is hypothesized that the LiS radical intermediate is generated during the final reaction and absorbed on the catalytic active site (Figure 10C). The final reaction consists of two elementary reactions:

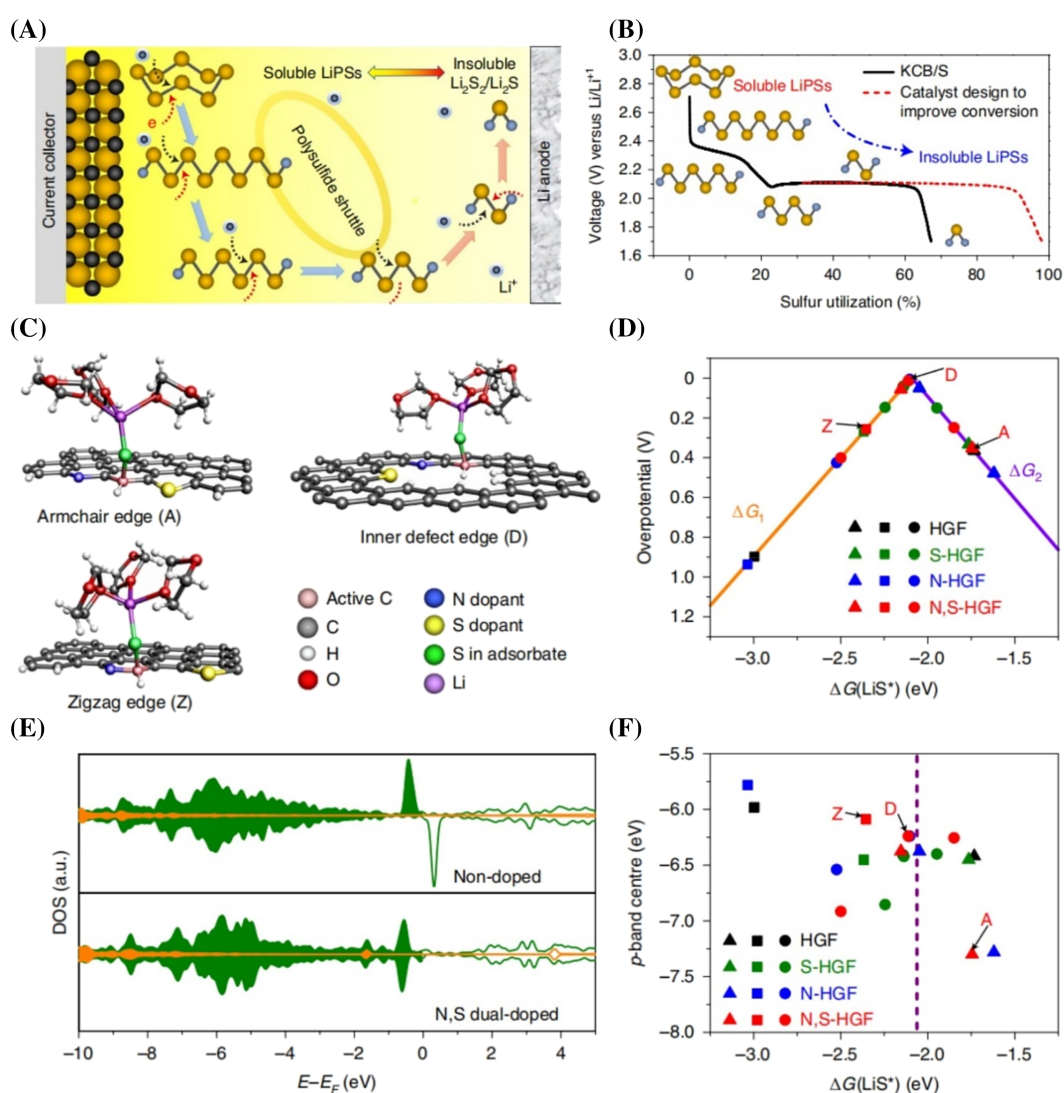
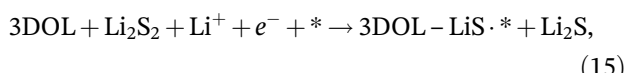
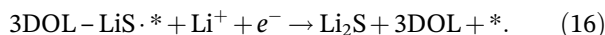


**FIGURE 10** Theoretical modeling on the activity origin of SRR: (A) Schematic diagram of the SRR process in Li-S chemistry. (B) Discharge profile of the standard Ketjen carbon black/sulfur (KCB/S) cathode. (C) Model configurations. (D) A volcano plot of the overpotential for the final step with the adsorption energies of the LiS radical intermediate on different active sites. (E) The alteration of PDOS and p-band center shift upon dual elements doping. (F) The relation between the p-band center and radical adsorption energy at different active carbons. Reproduced with permission of reference 82. Copyright 2020. Springer



Second, the overpotentials are determined by the rate-determining step, which is the least exothermic step. Taking these considerations into account,  $\eta$  can be expressed as:

$$\eta = E_0 - \max(\Delta U_i), \quad (17)$$

where  $E_0$  represents the equilibrium potential and  $\Delta U_i$  is the potential of elementary reaction. The potential of steps 15 and 16 (denoted as  $\Delta U_1$  and  $\Delta U_2$ ) can be written as:

$$\Delta U_1 = -\Delta G_1/e, \quad (18)$$

$$\Delta U_2 = -\Delta G_2/e. \quad (19)$$

The Gibbs free energy of each elementary step is functionally related to  $\Delta G(\text{LiS}\cdot^*)$ :

$$\Delta G_1 = \Delta G(\text{LiS}\cdot^*), \quad (20)$$

$$\Delta G_2 = -\Delta G(\text{LiS}\cdot^*) + 2G(\text{Li}_2\text{S}) - 2G(\text{Li}) - G(\text{Li}_2\text{S}_2). \quad (21)$$

Therefore, a volcano plot of overpotential as a function of  $\Delta G(\text{LiS}\cdot^*)$  is established as the catalytic model (Figure 10D), which becomes a key indicator for assessing the effects of materials on catalytic activity during SRR.

Finally, the influence of heteroatom on the catalytic SRR activities can be unraveled by the position of the  $p$  orbital of catalytic carbon, as the  $p$  orbital of the S atom in LiS radical is relatively constant. Heteroatom doping tunes the position of the  $p$  orbital of the active carbon in the PDOS and thereby manipulates the adsorption. Therefore, the  $p$ -band center of PDOS in carbon materials is regarded as the descriptor, which simplifies the evaluation process only by a rough calculation (Figure 10E,F). SRR catalytic model may shed light on the origin of the electrocatalyst and provide a guide to assess the catalytic activity of host materials.

With increasing requirements in Li-S batteries, it is challenging to understand the electrocatalysis of sulfur cathodes from an in-depth perspective based on current experimental techniques. Emerging theoretical models could elaborate on the issues of electrocatalysts from different perspectives. However, these models cannot individually investigate the complicated electrocatalytic processes, which include the adsorption, the electron transfer, and the redox reaction. These processes are closely related and each step affects the entire process. For example, the adsorption is an initiated step in the subsequent catalytic process but only the

adsorption strength is not sufficient as a criterion for evaluation. Strong adsorption immobilizes the LiPSs on the surface but causes some difficulties in the desorption of insoluble polysulfides, resulting in 2D deposition on the surface that is detrimental to further electrocatalysis reactions. The electron transfer kinetics also influences the activity of electrocatalysts, which depends on the smoothness of the electron transfer channel. A single adsorption model hardly clarifies these complexities of electrocatalysts. Therefore, combining the adsorption model with the decomposition model and SRR model could comprehensively assess the adsorption, electron transfer, and catalytic ability of a material. Moreover, the catalytic activity is associated with the intrinsic electronic properties of electrocatalysts, which largely determines the adsorption strength and barriers of redox reaction. Their relevance facilitates the rational integration of these models for exploring the fundamental principles of electrocatalysis. Especially,  $d$ - and  $p$ -band center models can be used to provide design strategies, while the simulated adsorption and catalytic capacity of the materials in Li-S batteries, in turn, validates the feasibility of  $d$ - and  $p$ -band center model, by evaluating the corresponding properties.

### 3 | APPLICATIONS OF THEORETICAL MODELS

Nowadays, theoretical simulations have become an increasingly powerful tool for understanding the mechanism in Li-S batteries, such as exploration for unsolved suspicions, design strategies, and high-throughput screening. Next, we will exhibit the applications of theoretical models from three aspects: (1) investigation of fundamentals in experiments; (2) rational design of high-performance electrocatalyst; and (3) applications of high throughput screening and machine learning.

#### 3.1 | Mechanism investigation

Despite there being some experimental evidence to explore the conversion of LiPSs like adsorption experiment, cyclic voltammetry experiment, and microstructure characterization (FESEM, XPS, etc.), the intrinsic mechanism of the conversion kinetics by electrocatalysts are still unclear. It is unfavorable for improving the reaction kinetics of LiPSs conversion in Li-S battery systems. As a promising alternative, theoretical models could address these challenging issues.

As an example, molybdenum disulfide ( $\text{MoS}_2$ ) and sulfur-deficient  $\text{MoS}_{2-x}$  have been applied as electrocatalysts due to their high electrochemical activity for several important reactions such as the hydrogen

evolution reaction (HER),<sup>124–126</sup> carbon dioxide conversion,<sup>127</sup> the oxygen evolution reaction (OER) and the oxygen reduction reaction (ORR).<sup>128,129</sup> MoS<sub>2</sub> and sulfur deficiencies MoS<sub>2-x</sub> were selected as host materials to catalyze the polysulfide conversion in a sulfur cathode (Figure 11A).<sup>130</sup> Generally, sulfur-deficient MoS<sub>2-x</sub> exhibits stronger catalytic activity than MoS<sub>2</sub>. However, it is difficult to illuminate the origin of improved electrocatalytic performance of MoS<sub>2-x</sub> compared to that of MoS<sub>2</sub> by experiments. Therefore, Zhang and coworkers carried out a systematic theoretical study on the discharge process from S<sub>8</sub> to Li<sub>2</sub>S on MoS<sub>2</sub> and sulfur deficiencies MoS<sub>2-x</sub> to explore the fundamental mechanism (Figure 11B).<sup>53</sup> Although the process and rate-determining step are identical for polysulfide conversion on MoS<sub>2</sub> and MoS<sub>2-x</sub>, the conversion on MoS<sub>2-x</sub> is thermodynamically more favorable than that

on MoS<sub>2</sub>. The underlying reason is the large charge densities of S atoms in MoS<sub>2-x</sub> induced by the sulfur deficiency, which enhances the interaction with polysulfides. The enhanced interaction endows MoS<sub>2-x</sub> with more thermodynamic and kinetic driving force for the electrocatalytic reaction than MoS<sub>2</sub>. The simulation results illustrate satisfactorily the catalytic effect of sulfur deficiencies in MoS<sub>2-x</sub>.

Furthermore, theoretical simulations could elucidate how the synergistic effects induced by a compound cathode speed up the polysulfide conversion. Cai, Long, and coworkers assembled a cathode scaffold with La<sub>2</sub>O<sub>3</sub> nanoparticles decorating on nitrogen-enriched mesoporous carbon (NMC/La<sub>2</sub>O<sub>3</sub>),<sup>131</sup> whose favorable performance is attributed to the synergistic effects of the mesopores, nitrogen doping, and La<sub>2</sub>O<sub>3</sub> nanoparticles. La<sub>2</sub>O<sub>3</sub> facilitates electron transfer and conversion kinetics in the course of the

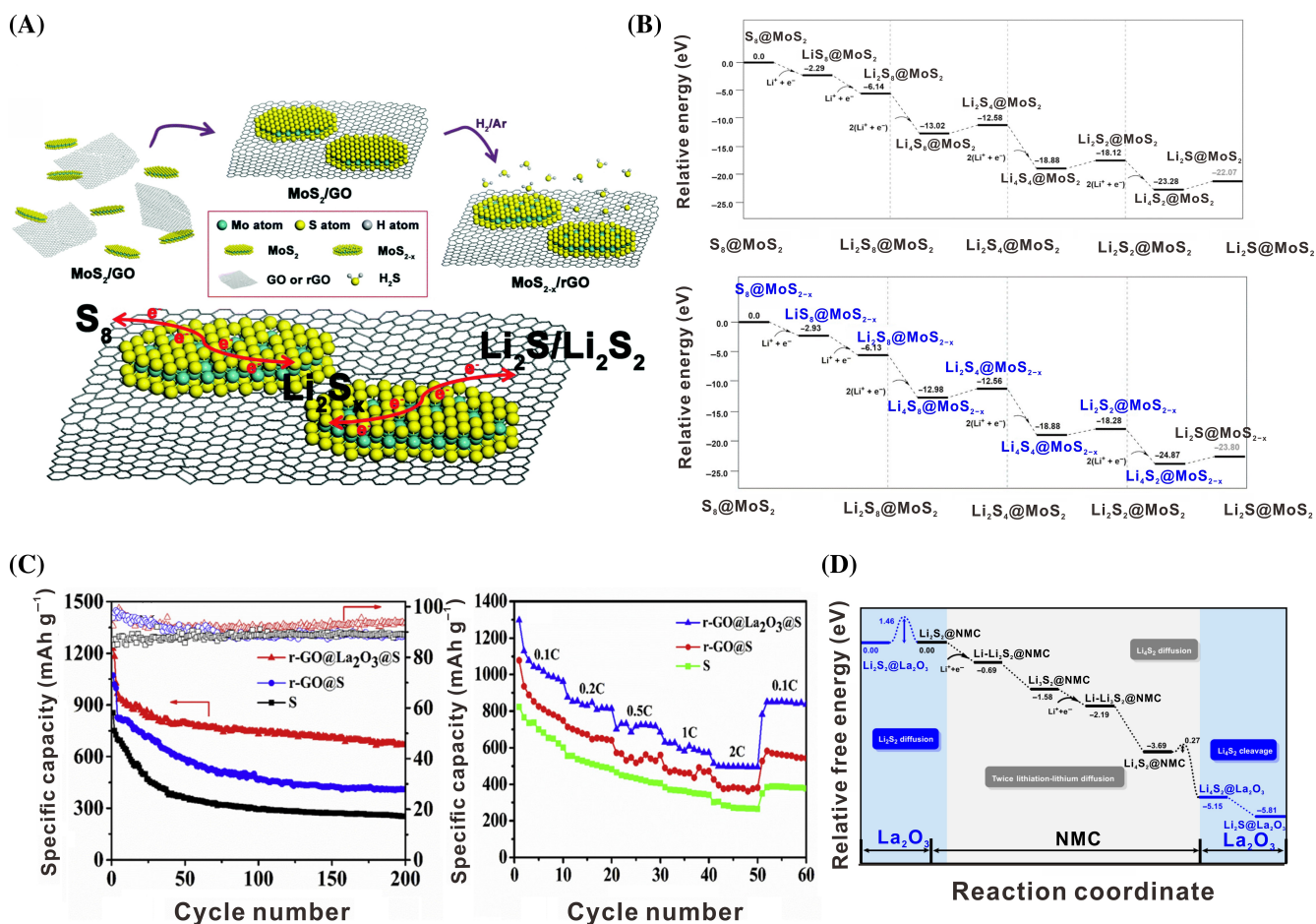


**FIGURE 11** Application of theoretical models for explaining the experimental phenomena. (A) Excellent electrochemical performance and enhanced polysulfide conversion kinetics of the sulfur-deficient MoS<sub>2-x</sub> in cathode material of the Li-S batteries. Reproduced with permission of reference 130. Copyright 2017. The Royal Society of Chemistry. (B) Relative energy profiles of polysulfide conversion mechanism on MoS<sub>2</sub>(001) and MoS<sub>2-x</sub>(001) surfaces. Reproduced with permission of reference 53. Copyright 2019. Elsevier. (C) High-performance Li-S batteries fabricated from the r-GO@La<sub>2</sub>O<sub>3</sub>@S composite. Reproduced with permission of reference 131. Copyright 2019. Elsevier. (D) Theoretical investigation of the synergistic effects of La<sub>2</sub>O<sub>3</sub> and nitrogen-doped carbon for improved redox kinetics. Reproduced with permission of reference 132. Copyright 2021. Elsevier

discharge process due to smooth polysulfide migration and rapid cleavage of polysulfide dimer, while the nitrogen-doped carbon provides a channel for polysulfide dimer migrating rapidly based on a systematically theoretical simulation (Figure 11C,D).<sup>132</sup> The investigations of catalytic mechanisms deepen the understanding and inspire the innovation of electrocatalysts in Li-S batteries.

### 3.2 | Design strategies

Theoretical models could also provide reasonable strategies to upgrade the performance of the original S cathode in batteries, such as atomic surface functionalization, heteroatomic doping, and band tuning strategy.

Recently, 2D transition metal carbides and nitrides (MXenes) have been utilized as electrocatalysts in Li-S batteries due to their unique 2D structures, abundant surface functional groups, and high electrical conductivities.<sup>108,133–135</sup> As the binding strength and catalytic activity of MXenes can be regulated by altering the surface functional terminations, a general atomic surface modification strategy is proposed to modulate the anchoring and electrocatalytic behavior. Cui and coworkers introduced a series of surface terminating groups, including N, P, O, S, F, and Cl, onto  $\text{Ti}_3\text{C}_2$  (Figure 12A).<sup>136</sup> All modified  $\text{Ti}_3\text{C}_2$  remains excellent metallic conductivity as the majority of electronic states at the Fermi level are uninfluenced by terminating groups. While the MXenes functionalized by O and S groups exhibit favorable catalytic performance due to moderate surface adsorption strength and reduced  $\text{Li}_2\text{S}$  decomposition barrier. Therefore, a suitable modification strategy not only retains the advantages of electrocatalysts but also boosts the electrochemical performance of Li-S batteries.

Heteroatom doping is another strategy to modulate surface performance by converting surface polarity and regulating active sites for catalytic conversion.<sup>141</sup> Various Lewis acidic or basic heteroatoms were embedded on the black phosphorus (BP) surface to enhance its performance (Figure 12B).<sup>137</sup> All the adsorption capacities of doped BP hosts improve regardless of the type of heteroatoms. However, Lewis acidic atom-doped BP plays a positive effect on the polysulfide conversion whereas Lewis's basic N-doped BP hinders the conversion. It is mainly attributed to the formation of a “frustrated Lewis pair” between Lewis acidic doped atom and Lewis basic P atom.

Moreover, modulating the energy gap between bonding and antibonding orbitals, which facilitates the electron transfer and LiPSs transformation kinetics, has been widely applied to designing host materials. For example, the alteration of cations in sulfide could modulate the hybridization of

$d-p$  orbital between metal in disulfide and sulfur in LiPSs.<sup>138</sup> The calculation results show that W cation promotes the hybridization of  $d-p$  orbitals and decreases the energy gap between bonding and antibonding orbitals. The reduced gap facilitates the electron transfer and thereby promotes the LiPSs interfacial redox reactions (Figure 12C). The prepared  $\text{WS}_2$  with nitrogen-doped carbon ( $\text{WS}_2@\text{NC}$ ) composite exhibits excellent performance compared to other sulfide materials. Furthermore,  $d-p$  orbital hybridization between the transition metal and the sulfur species is regarded as a descriptor to guide the screening and design of suitable single-atom catalysts (SACs) in Li-S batteries (Figure 12D).<sup>139</sup> According to the simulation results, the adsorption and electrocatalysis of LiPSs on SACs can be modulated by substituting different individual metal atoms. The transition metal with a lower atomic number is considered to be embedded in the carbon frame because of few electrons filled with antibonding states. Finally, the single-atom Ti is selected with the assistance of theoretical calculations and has the best electrochemical performance among the transition metal candidates. Moreover, Wang's group compared the DOS of  $\text{Fe}_3\text{O}_4$  and FeP and demonstrated that regulating  $d-p$  band centers of host materials could adjust the electronic exchange and promote LiPSs redox kinetics (Figure 12E).<sup>140</sup>

### 3.3 | High-throughput screening and machine learning

Lately, high-throughput first-principles calculations and machine learning empower rapid searching for promising catalyst candidates by studying the adsorption properties, energy barriers of decomposition and diffusion, and band gaps, which observably lower the cost of trials and errors.<sup>33,142,143</sup>

To screen rational catalyst candidates, Cui's group performed high-throughput calculations and successfully synthesized large-scale SACs under the guidance of DFT calculations.<sup>144</sup> Initially, the energy barriers of decomposition and diffusion of  $\text{Li}_2\text{S}$  on a series of SAC materials, including graphene, and single atom Fe, Mn, Ru, Zn, Co, Cu, V, and Ag on N-doped graphene (NG), were calculated. Vanadium single atom on NG is then targeted as a promising cathode for Li-S batteries since the lowest decomposition barrier (1.10 eV) among all the investigated SAC materials. Finally, the significant enhancement for the catalytic performance of synthesized single atoms vanadium catalyst verified the availability of the high-throughput simulations (Figure 13A).

The synergistic effects between SAC and N-doped carbon materials expedite the practical process of the supported SACs on NG as the cathode of Li-S battery.

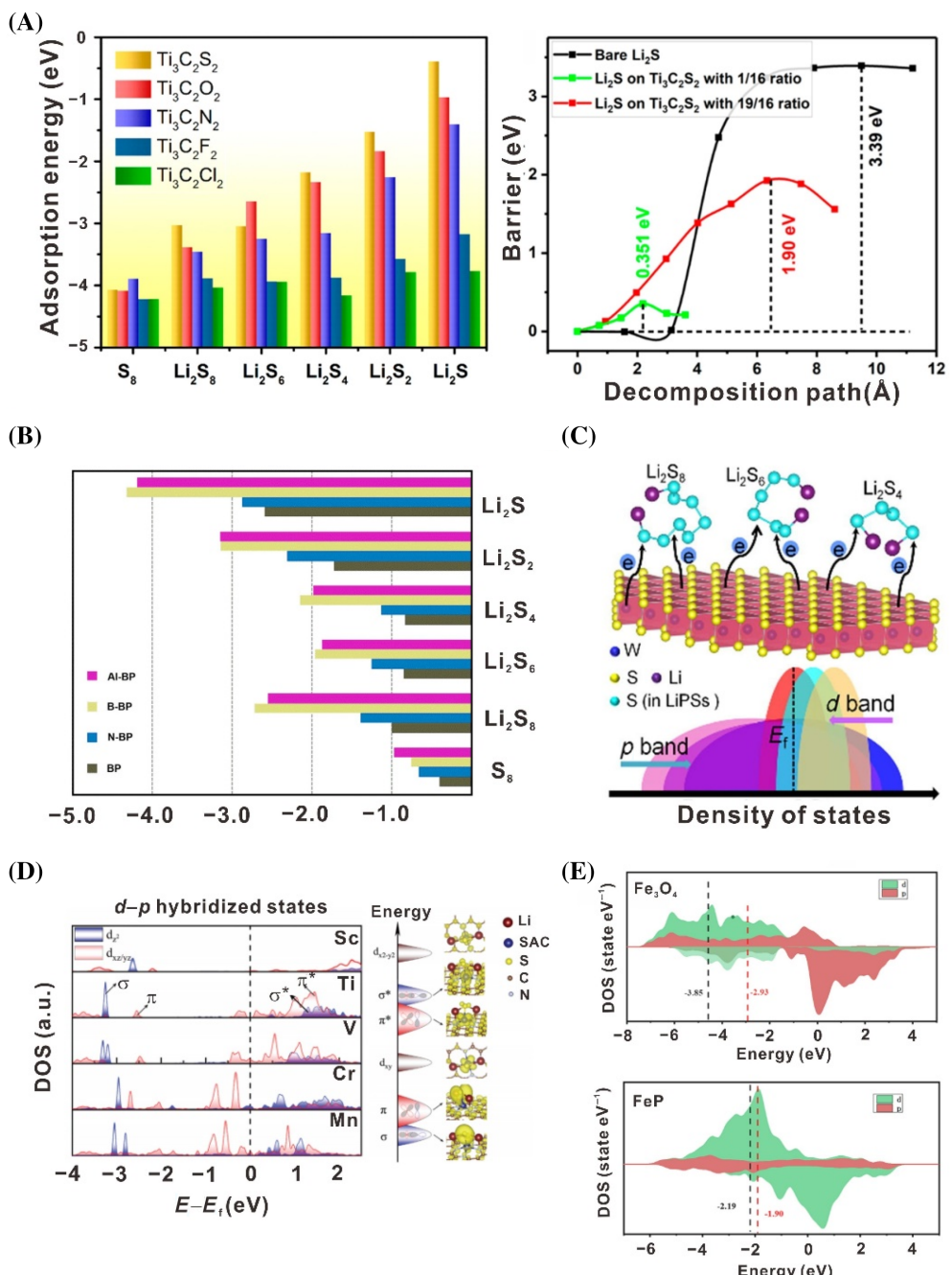


**FIGURE 12** Modification strategies proposed by theoretical simulations. (A) Atomic surface functional strategy for Ti<sub>3</sub>C<sub>2</sub>T<sub>2</sub> MXene in Li-S batteries. Reproduced with permission of reference 136. Copyright 2019. American Chemical Society. (B) Heteroatom doping strategy on the BP surface. Reproduced with permission of reference 137. Copyright 2020. Elsevier. (C) Modulating the energy gap of various disulfide@NC. Reproduced with permission of reference 138. Copyright 2021. Elsevier. (D) The descriptor of d-p orbital hybridization between the transition metal and the sulfur species for single-atom catalysts in Li-S batteries. Reproduced with permission of reference 139. Copyright 2021. Wiley-VCH. (E) Dual-functional materials obtained by regulating d-p band centers. Reproduced with permission of reference 140. Copyright 2021. Elsevier

However, the combinations of supported SAC on NG are tremendous, which exceeds the scope of conventional trials or general DFT calculations. The bottleneck issue when screening the optimal combination of SACs can be overcome effectively by machine-learning studies based on high-throughput calculations (Figure 13B,C).<sup>145,146</sup> Li's

group conducted an unbiased evaluation of SACs including 3d, 4d, and 5d transition metals by the machine-learning classification and regression within the frame of Crystal Graph Convolutional Neural Networks (CGCNN).<sup>147,148</sup> The S-S bond breaking in polysulfides is used to classify the adsorption categories of electrocatalysts as it is the first step

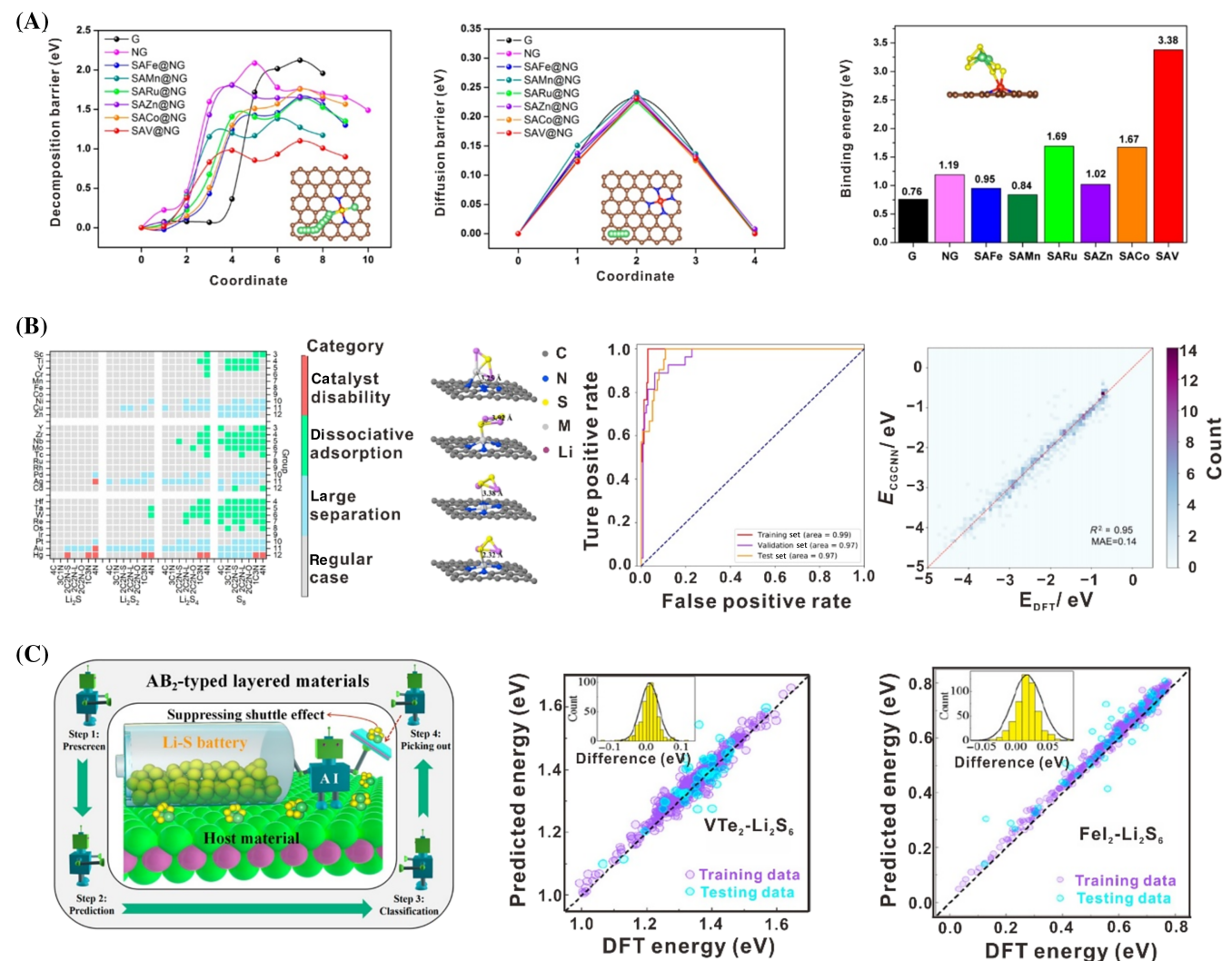


**FIGURE 13** High-throughput calculations and machine learning for screening suitable electrocatalysts. (A) Synthesized single atom vanadium catalysts under the guidance of theoretical calculation with fast kinetic and long-life in Li-S Batteries. Reproduced with permission of reference 144. Copyright 2020. American Chemical Society. (B) The design strategy of single atomic cathode catalysts by machine learning. Reproduced with permission of reference 145. Copyright 2021. American Chemical Society. (C) Machine learning method for screening AB<sub>2</sub>-type sulfur host material. Reproduced with permission of reference 146. Copyright 2021. American Chemical Society

for SRR. The adsorption ability of LiS radical is one of the indicators to predict the catalytic activity of SACs based on SRR catalytic models and results of machine learning. A series of descriptors accelerate the screening of catalysts and provide a guide that the appropriate SACs should balance the adsorption and electrocatalytic performance rationally.

Based on the available data regarding materials, Zhang and coworkers also combined DFT calculations with machine learning for rapid screening of two-dimensional layered materials (AB<sub>2</sub>-type materials) in Li-S batteries (Figure 13C). A workflow was constructed via prescreening from the 2DMatPedia database<sup>149</sup> and classification using the extreme gradient boosting (XGBoost) algorithm to accelerate the discovery of host materials. The most promising AB<sub>2</sub>-type host materials are identified

from the perspective of adsorptions and electron transportation (larger than 1.0 eV adsorption energies for LiPSs and appreciable electron transportation capability). Notably, the accuracy of machine-learning methods is comparable to that of DFT; while the prediction time shortens sharply.

## 4 | CONCLUSION AND OUTLOOK

Theoretical models have become indispensable tools in the study of Li-S batteries. Characterization methods can reflect the overall performance of Li-S batteries while theoretical simulations can afford mechanistic insights at the atomic level. Combined experiments and theoretical

models could introduce a deep understanding of the internal mechanism for host materials. A summary of future applications of theoretical models in S cathode materials is discussed as follows.

Although there have been tremendous studies on the modification of various S host materials, a comprehensive understanding of a wide range of host materials could be helpful to single out promising materials to suppress the shuttle effect in Li–S batteries. Theoretical models are powerful tools to accelerate the recognition of the correlation between host materials and the electrochemical performance of batteries. For example, the binding ability can be evaluated by adsorption models, and catalytic abilities can be judged by the energy barrier of Li diffusion,  $\text{Li}_2\text{S}$  decomposition, and sulfur reduction model. In addition, *d*- and *p*-band center models could illustrate the intrinsic difference for the conversion reaction on various materials at the electronic level. The theoretical tools are available for deeply probing the fundamental mechanisms of S redox reaction at the atomic level and further designing host materials.

Furthermore, except to exploring the mechanism and design materials, high-throughput screening and machine learning are promising applications in the study of Li–S batteries. The data-driven methods on basis of theoretical models present tremendous potentials in accurately predicting material properties such as adsorption energy. Especially, the innovative technology liberates the discovery of energy materials from repetitive and tedious experiments and resists the restriction of the capabilities of routine DFT calculations.

The charge and discharge process in Li–S batteries involves a series of sulfur species as reaction intermediates, which is difficult to be characterized by experimental methods. It seems impossible to describe the intrinsic mechanism of the charge and discharge process on various S hosts based on current technology. Fortunately, with the development of calculation technology, these indistinct and fundamental mechanisms are being investigated elaborately. The theoretical simulations will gain extensive applications and introduce revolutions to the research paradigm of Li–S batteries: diversified descriptors, general laws, and unambiguous charge–discharge mechanism. It is believed that the practical process of Li–S batteries will be sped up with the assistance of theoretical simulations.

## ACKNOWLEDGMENTS

This work was supported by Beijing Municipal Natural Science Foundation (Z200011), National Natural Science Foundation of China (22109086 and 21825501), and Taian Municipal Technology Foundation (2019GX049). Xiang Chen appreciates the support from the Shuimu Tsinghua Scholar Program of Tsinghua University. The

authors acknowledged the support from Tsinghua National Laboratory for Information Science and Technology for theoretical simulations.

## CONFLICT OF INTEREST

The authors declare no conflict of interest.

## ORCID

Shuai Feng  <https://orcid.org/0000-0002-8604-2097>

Zhong-Heng Fu  <https://orcid.org/0000-0001-8779-9086>

Xiang Chen  <https://orcid.org/0000-0002-7686-6308>

Qiang Zhang  <https://orcid.org/0000-0002-3929-1541>

## REFERENCES

- Dörfler S, Althues H, Härtel P, Abendroth T, Schumm B, Kaskel S. Challenges and key parameters of lithium–sulfur batteries on pouch cell level. *Joule*. 2020;4(3):539–554.
- Pang Q, Liang X, Kwok CY, Nazar LF. Review—the importance of chemical interactions between sulfur host materials and lithium polysulfides for advanced lithium–sulfur batteries. *J Electrochem Soc*. 2015;162(14):A2567-A2576.
- Peng H-J, Huang J-Q, Cheng X-B, Zhang Q. Review on high-loading and high-energy lithium–sulfur batteries. *Adv Energy Mater*. 2017;7(24):1700260.
- Hong X, Wang R, Liu Y, Fu J, Liang J, Dou S. Recent advances in chemical adsorption and catalytic conversion materials for Li–S batteries. *J Energy Chem*. 2020;42:144–168.
- Lei J, Liu T, Chen J, et al. Exploring and understanding the roles of  $\text{Li}_2\text{S}_n$  and the strategies to beyond present Li–S batteries. *Chem*. 2020;6(10):2533–2557.
- Liu X, Li Y, Xu X, Zhou L, Mai L. Rechargeable metal (Li, Na, Mg, Al)-sulfur batteries: materials and advances. *J Energy Chem*. 2021;61:104–134.
- Liu J, Yuan H, Tao X, et al. Recent progress on biomass-derived ecomaterials toward advanced rechargeable lithium batteries. *EcoMat*. 2020;2(1):e12019.
- Kong L, Tang C, Peng H-J, Huang JQ, Zhang Q. Advanced energy materials for flexible batteries in energy storage: a review. *SmartMat*. 2020;1(1):1–35.
- Chen X, Li H-R, Shen X, Zhang Q. The origin of the reduced reductive stability of ion–solvent complexes on alkali and alkaline earth metal anodes. *Angew Chem Int Ed*. 2018;57(51):16643–16647.
- Sakai M. A reaction model for Li deposition at the positive electrode of the Braga–Goodenough Li–S battery. *J Electrochem Soc*. 2020;167(16):160540.
- Ji X, Nazar LF. Advances in Li–S batteries. *J Mater Chem*. 2010;20(44):9821–9826.
- Kumar R, Liu J, Hwang J-Y, Sun Y-K. Recent research trends in Li–S batteries. *J Mater Chem A*. 2018;6(25):11582–11605.
- Wang Y, Huang X, Zhang S, Hou Y. Sulfur hosts against the shuttle effect. *Small Methods*. 2018;2(6):1700345.
- Kaiser MR, Han Z, Liang J, Dou SX, Wang J. Lithium sulfide-based cathode for lithium-ion/sulfur battery: recent progress and challenges. *Energy Storage Mater*. 2019;19:1–15.
- Ng SF, Lau M, Ong W-J. Lithium–sulfur battery cathode design: tailoring metal-based nanostructures for robust polysulfide adsorption and catalytic conversion. *Adv Mater*. 2021;33(50):2008654.

16. Wang P, Xi B, Huang M, Chen W, Feng J, Xiong S. Emerging catalysts to promote kinetics of lithium–sulfur batteries. *Adv Energy Mater.* 2021;11(7):2002893.
17. Du L, Wang H, Yang M, et al. Free-standing nanostructured architecture as a promising platform for high-performance lithium–sulfur batteries. *Small Struct.* 2020;1(3):2000047.
18. Subramaniam A, Kolluri S, Santhanagopalan S, Subramanian VR. An efficient electrochemical-thermal tanks-in-series model for lithium-ion batteries. *J Electrochem Soc.* 2020;167(11):113506.
19. Agostini M, Scrosati B, Hassoun J. An advanced lithium-ion sulfur battery for high energy storage. *Adv Energy Mater.* 2015;5(16):1500481.
20. Boyd DA. Sulfur and its role in modern materials science. *Angew Chem Int Ed.* 2016;55(50):15486-15502.
21. Chung S-H, Manthiram A. Current status and future prospects of metal–sulfur batteries. *Adv Mater.* 2019;31(27):1901125.
22. Su D, Cortie M, Wang G. Fabrication of N-doped graphene–carbon nanotube hybrids from prussian blue for lithium–sulfur batteries. *Adv Energy Mater.* 2017;7(8):1602014.
23. Zhao M, Li B-Q, Peng H-J, Yuan H, Wei JY, Huang JQ. Lithium–sulfur batteries under lean electrolyte conditions: challenges and opportunities. *Angew Chem Int Ed.* 2020;59(31):12636-12652.
24. Maurer C, Commerell W, Hintennach A, Jossen A. Continuous shuttle current measurement method for lithium sulfur cells. *J Electrochem Soc.* 2020;167(9):090534.
25. Liu B, Fang R, Xie D, et al. Revisiting scientific issues for industrial applications of lithium–sulfur batteries. *Energ Environ Sci.* 2018;1(4):196-208.
26. Huang L, Li J, Liu B, et al. Electrode design for lithium–sulfur batteries: problems and solutions. *Adv Funct Mater.* 2020;30(22):1910375.
27. Song Y-W, Peng Y-Q, Zhao M, et al. Understanding the impedance response of lithium polysulfide symmetric cells. *Small Sci.* 2021;1(11):2100042.
28. Kong L, Yin L, Xu F, et al. Electrolyte solvation chemistry for lithium–sulfur batteries with electrolyte-lean conditions. *J Energy Chem.* 2021;55:80-91.
29. Zhang Y, Zhang P, Zhang S, et al. A flexible metallic TiC nanofiber/vertical graphene 1D/2D heterostructured as active electrocatalyst for advanced Li–S batteries. *InfoMat.* 2021;3(7):790-803.
30. Geng C, Hua W, Wang D, Ling G, Zhang C, Yang Q-H. Demystifying the catalysis in lithium–sulfur batteries: characterization methods and techniques. *SusMat.* 2021;1(1):51-65.
31. Zhao C-X, Chen W-J, Zhao M, et al. Redox mediator assists electron transfer in lithium–sulfur batteries with sulfurized polyacrylonitrile cathodes. *EcoMat.* 2021;3(1):e12066.
32. Yao Y-X, Zhang X-Q, Li B-Q, et al. A compact inorganic layer for robust anode protection in lithium–sulfur batteries. *InfoMat.* 2020;2(2):379-388.
33. Zha C, Wu D, Gu X, Chen H. Triple-phase interfaces of graphene-like carbon clusters on antimony trisulfide nanowires enable high-loading and long-lasting liquid Li<sub>2</sub>S<sub>6</sub>-based lithium–sulfur batteries. *J Energy Chem.* 2021;59:599-607.
34. Zhang X-Q, Jin Q, Nan Y-L, et al. Electrolyte structure of lithium polysulfides with anti-reductive solvent shells for practical lithium–sulfur batteries. *Angew Chem Int Ed.* 2021;60(28):15503-15509.
35. Chen W-J, Li B-Q, Zhao C-X, et al. Electrolyte regulation towards stable lithium–metal anodes in lithium–sulfur batteries with sulfurized polyacrylonitrile cathodes. *Angew Chem Int Ed.* 2020;59(27):10732-10745.
36. Wang Q, Zhao H, Li B, et al. MOF-derived Co<sub>9</sub>S<sub>8</sub> nano-flower cluster array modified separator towards superior lithium sulfur battery. *Chin Chem Lett.* 2021;32(3):1157-1160.
37. Zhou X, Liu T, Zhao G, Yang X, Guo H. Cooperative catalytic interface accelerates redox kinetics of sulfur species for high-performance Li–S batteries. *Energy Storage Mater.* 2021;40:139-149.
38. Xie J, Peng H-J, Song Y-W, et al. Spatial and kinetic regulation of sulfur electrochemistry on semi-immobilized redox mediators in working batteries. *Angew Chem Int Ed.* 2020;59(40):17670-17675.
39. Emerce NB, Eroglu D. Effect of electrolyte-to-sulfur ratio in the cell on the Li–S battery performance. *J Electrochem Soc.* 2019;166(8):A1490-A1500.
40. Raccichini R, Furness L, Dibden JW, Owen JR, Garcia-Araez N. Impedance characterization of the transport properties of electrolytes contained within porous electrodes and separators useful for Li–S batteries. *J Electrochem Soc.* 2018;165(11):A2741-A2749.
41. Yan C, Zhang X-Q, Huang J-Q, Liu Q, Zhang Q. Lithium-anode protection in lithium–sulfur batteries. *Trends Chem.* 2019;1(7):693-704.
42. Jayaprakash N, Shen J, Moganty SS, Corona A, Archer LA. Porous hollow carbon@sulfur composites for high-power lithium–sulfur batteries. *Angew Chem Int Ed.* 2011;50(26):5904-5908.
43. Guo J, Xu Y, Wang C. Sulfur-impregnated disordered carbon nanotubes cathode for lithium–sulfur batteries. *Nano Lett.* 2011;11(10):4288-4294.
44. Liang C, Dudney NJ, Howe JY. Hierarchically structured sulfur/carbon nanocomposite material for high-energy lithium battery. *Chem Mater.* 2009;21(19):4724-4730.
45. Lu R, Cheng M, Mao L, et al. Nitrogen-doped nanoarray-modified 3D hierarchical graphene as a cofunction host for high-performance flexible Li–S battery. *EcoMat.* 2020;2(1):e12010.
46. Li Q, Song Y, Xu R, et al. Biотemplating growth of nepenthes-like N-doped graphene as a bifunctional polysulfide scavenger for Li–S batteries. *ACS Nano.* 2018;12(10):10240-10250.
47. Chen S, Huang X, Liu H, et al. 3D hyperbranched hollow carbon nanorod architectures for high-performance lithium–sulfur batteries. *Adv Energy Mater.* 2014;4(8):1301761.
48. Wang J, Yang H, Chen Z, et al. Double-shelled phosphorus and nitrogen codoped carbon nanospheres as efficient polysulfide mediator for high-performance lithium–sulfur batteries. *Adv Sci.* 2018;5(11):1800621.
49. Fang L, Feng Z, Cheng L, Winans RE, Li T. Design principles of single atoms on carbons for lithium–sulfur batteries. *Small Methods.* 2020;4(10):2000315.
50. He J, Chen Y, Manthiram A. Vertical Co<sub>9</sub>S<sub>8</sub> hollow nanowall arrays grown on a Celgard separator as a multifunctional polysulfide barrier for high-performance Li–S batteries. *Energ Environ Sci.* 2018;11(9):2560-2568.
51. Tao X, Wang J, Liu C, et al. Balancing surface adsorption and diffusion of lithium-polysulfides on nonconductive oxides for lithium–sulfur battery design. *Nat Commun.* 2016;7(1):11203.
52. Zhang J, Hu H, Li Z, Lou XWD. Double-shelled nanocages with cobalt hydroxide inner shell and layered double

- hydroxides outer shell as high-efficiency polysulfide mediator for lithium–sulfur batteries. *Angew Chem Int Ed.* 2016;55(12):3982–3986.
53. Zhang Q, Zhang X, Li M, Liu J, Wu Y. Sulfur-deficient  $\text{MoS}_{2-x}$  promoted lithium polysulfides conversion in lithium–sulfur battery: a first-principles study. *Appl Surf Sci.* 2019;487:452–463.
54. Li J, Niu Z, Guo C, Li M, Bao W. Catalyzing the polysulfide conversion for promoting lithium sulfur battery performances: a review. *J Energy Chem.* 2021;54:434–451.
55. Zhao M, Peng H-J, Li B-Q, et al. Electrochemical phase evolution of metal-based pre-catalysts for high-rate polysulfide conversion. *Angew Chem Int Ed.* 2020;132(23):9096–9102.
56. Lim W-G, Kim S, Jo C, Lee J. A comprehensive review of materials with catalytic effects in Li–S batteries: enhanced redox kinetics. *Angew Chem Int Ed.* 2019;58(52):18746–18757.
57. Du Z, Chen X, Hu W, et al. Cobalt in nitrogen-doped graphene as single-atom catalyst for high-sulfur content lithium–sulfur batteries. *J Am Chem Soc.* 2019;141(9):3977–3985.
58. Xu Z-L, Lin S, Onofrio N, et al. Exceptional catalytic effects of black phosphorus quantum dots in shuttling-free lithium sulfur batteries. *Nat Commun.* 2018;9(1):4164.
59. Park J, Yu B-C, Park JS, et al. Tungsten disulfide catalysts supported on a carbon cloth interlayer for high performance Li–S battery. *Adv Energy Mater.* 2017;7(11):1602567.
60. Bi C-X, Zhao M, Hou L-P, et al. Anode material options toward 500 Wh kg<sup>-1</sup> lithium–sulfur batteries. *Adv Sci.* 2021;9(2):2103910.
61. Zhao C-X, Li X-Y, Zhao M, et al. Semi-immobilized molecular electrocatalysts for high-performance lithium–sulfur batteries. *J Am Chem Soc.* 2021;143(47):19865–19872.
62. Wang T, Luo D, Zhang Y, et al. Hierarchically porous  $\text{Ti}_3\text{C}_2$  MXene with tunable active edges and unsaturated coordination bonds for superior lithium–sulfur batteries. *ACS Nano.* 2021;15(12):19457–19467.
63. Chen P-Y, Yan C, Chen P, et al. Selective permeable lithium-ion channels on lithium metal for practical lithium–sulfur pouch cells. *Angew Chem Int Ed.* 2021;60(33):18031–18036.
64. Zhao M, Chen X, Li X-Y, Li BQ, Huang JQ. Lithium–sulfur batteries: an organodiselenide comediator to facilitate sulfur redox kinetics in lithium–sulfur batteries. *Adv Mater.* 2021;33(13):2170100.
65. Luo X, Lu X, Chen X, et al. A functional hyperbranched binder enabling ultra-stable sulfur cathode for high-performance lithium–sulfur battery. *J Energy Chem.* 2020;50:63–72.
66. Gao H, Ning S, Zou J, et al. The electrocatalytic activity of  $\text{BaTiO}_3$  nanoparticles towards polysulfides enables high-performance lithium–sulfur batteries. *J Energy Chem.* 2020;48:208–216.
67. Yao N, Chen X, Shen X, et al. An atomic insight into the chemical origin and variation of the dielectric constant in liquid electrolytes. *Angew Chem Int Ed.* 2021;60(39):21473–21478.
68. Xu R, Shen X, Ma X-X, et al. Identifying the critical anioncation coordination to regulate the electric double layer for an efficient lithium–metal anode interface. *Angew Chem Int Ed.* 2021;60(8):4215–4220.
69. Jayan R, Islam MM. Single-atom catalysts for improved cathode performance in Na–S batteries: a density functional theory (DFT) study. *J Phys Chem C.* 2021;125(8):4458–4467.
70. Ma X-X, Chen X, Bai Y-K, Shen X, Zhang R, Zhang Q. The defect chemistry of carbon frameworks for regulating the lithium nucleation and growth behaviors in lithium metal anodes. *Small.* 2021;17(48):2007142.
71. Fu Z-H, Chen X, Zhao C-Z, et al. Stress regulation on atomic bonding and ionic diffusivity: mechanochemical effects in sulfide solid electrolytes. *Energ Fuel.* 2021;35(12):10210–10218.
72. Wang L, Zhang T, Yang S, Cheng F, Liang J, Chen J. A quantum-chemical study on the discharge reaction mechanism of lithium–sulfur batteries. *J Energy Chem.* 2013;22(1):72–77.
73. Kamyab N, Coman PT, Madi Reddy SK, Santhanagopalan S, White RE. Mathematical model for Li–S cell with shuttling-induced capacity loss approximation. *J Electrochim Soc.* 2020;167(13):130532.
74. Ponce V, Seminario JM. Lithiation of sulfur-graphene compounds using reactive force-field molecular dynamics simulations. *J Electrochim Soc.* 2020;167(10):100555.
75. Kumaresan K, Mikhaylik Y, White RE. A mathematical model for a lithium–sulfur cell. *J Electrochim Soc.* 2008;155(8):A576–A582.
76. Chen X, Hou T, Persson KA, Zhang Q. Combining theory and experiment in lithium–sulfur batteries: current progress and future perspectives. *Mater Today.* 2019;22:142–158.
77. Li J, Qu Y, Chen C, Zhang X, Shao M. Theoretical investigation on lithium polysulfide adsorption and conversion for high-performance Li–S batteries. *Nanoscale.* 2021;13(1):15–35.
78. Zhou G, Tian H, Jin Y, et al. Catalytic oxidation of  $\text{Li}_2\text{S}$  on the surface of metal sulfides for Li–S batteries. *Proc Natl Acad Sci U S A.* 2017;114(5):840–845.
79. Balach J, Linnemann J, Jaumann T, Giebel L. Metal-based nanostructured materials for advanced lithium–sulfur batteries. *J Mater Chem A.* 2018;6(46):23127–23168.
80. Zeng P, Liu C, Cheng C, et al. Propelling polysulfide redox conversion by *d*-band modulation for high sulfur loading and low temperature lithium–sulfur batteries. *J Mater Chem A.* 2021;9(34):18526–18536.
81. Cheng Z, Pan H, Chen J, Meng X, Wang R. Separator modified by cobalt-embedded carbon nanosheets enabling chemisorption and catalytic effects of polysulfides for high-energy-density lithium–sulfur batteries. *Adv Energy Mater.* 2019;9(32):1901609.
82. Peng L, Wei Z, Wan C, et al. A fundamental look at electrocatalytic sulfur reduction reaction. *Nat Catal.* 2020;3(9):762–770.
83. Hao X, Ma J, Cheng X, et al. Electron and ion co-conductive catalyst achieving instant transformation of lithium polysulfide towards  $\text{Li}_2\text{S}$ . *Adv Mater.* 2021;33(52):2105362.
84. Wang S, Feng S, Liang J, et al. Insight into  $\text{MoS}_2$ – $\text{MoN}$  heterostructure to accelerate polysulfide conversion toward high-energy-density lithium–sulfur batteries. *Adv Energy Mater.* 2021;11(11):2003314.
85. Hu G, Xu C, Sun Z, et al. 3D graphene-foam-reduced-graphene-oxide hybrid nested hierarchical networks for high-performance Li–S batteries. *Adv Mater.* 2016;28(8):1603–1609.
86. Borchardt L, Oschatz M, Kaskel S. Carbon materials for lithium sulfur batteries—ten critical questions. *Chem Eur J.* 2016;22(22):7324–7351.
87. Liu H, Cheng X, Zhang R, et al. Mesoporous graphene hosts for dendrite-free lithium metal anode in working rechargeable batteries. *Trans Tianjin Univ.* 2020;26(2):127–134.

88. Hou T-Z, Xu W-T, Chen X, Peng H-J, Huang J-Q, Zhang Q. Lithium bond chemistry in lithium–sulfur batteries. *Angew Chem Int Ed*. 2017;56(28):8178–8182.
89. Hou T-Z, Peng H-J, Huang J-Q, Zhang Q, Li B. The formation of strong-couple interactions between nitrogen-doped graphene and sulfur/lithium (poly)sulfides in lithium–sulfur batteries. *2D Mater*. 2015;2(1):014011.
90. Wang Z, Dong Y, Li H, et al. Enhancing lithium–sulphur battery performance by strongly binding the discharge products on amino-functionalized reduced graphene oxide. *Nat Commun*. 2014;5(1):5002.
91. Zhou G, Zhao Y, Manthiram A. Dual-confined flexible sulfur cathodes encapsulated in nitrogen-doped double-shelled hollow carbon spheres and wrapped with graphene for Li–S batteries. *Adv Energy Mater*. 2015;5(9):1402263.
92. Cheng X-B, Huang J-Q, Zhang Q, Peng H-J, Zhao MQ, Wei F. Aligned carbon nanotube/sulfur composite cathodes with high sulfur content for lithium–sulfur batteries. *Nano Energy*. 2014;4:65–72.
93. Hou T-Z, Chen X, Peng H-J, et al. Design principles for heteroatom-doped nanocarbon to achieve strong anchoring of polysulfides for lithium–sulfur batteries. *Small*. 2016;12(24):3283–3291.
94. Chen X, Bai Y-K, Zhao C-Z, Shen X. Lithium bonds in lithium batteries. *Angew Chem Int Ed*. 2020;59(28):11192–11195.
95. Zhou G, Paek E, Hwang GS, Manthiram A. Long-life Li/polysulphide batteries with high sulphur loading enabled by lightweight three-dimensional nitrogen/sulphur-codoped graphene sponge. *Nat Commun*. 2015;6(1):7760.
96. Zhou G, Paek E, Hwang GS, Manthiram A. High-performance lithium–sulfur batteries with a self-supported, 3D  $\text{Li}_2\text{S}$ -doped graphene aerogel cathodes. *Adv Energy Mater*. 2016;6(2):1501355.
97. Tao Y, Wei Y, Liu Y, et al. Kinetically-enhanced polysulfide redox reactions by  $\text{Nb}_2\text{O}_5$  nanocrystals for high-rate lithium–sulfur battery. *Energ Environ Sci*. 2016;9(10):3230–3239.
98. Wang Y, Li M, Xu L, et al. Polar and conductive iron carbide@N-doped porous carbon nanosheets as a sulfur host for high performance lithium sulfur batteries. *Chem Eng J*. 2019;358:962–968.
99. Li N, Xu Z, Wang P, et al. High-rate lithium–sulfur batteries enabled via vanadium nitride nanoparticle/3D porous graphene through regulating the polysulfides transformation. *Chem Eng J*. 2020;398:125432.
100. Li R, Peng H, Wu Q, et al. Sandwich-like catalyst–carbon–catalyst trilayer structure as a compact 2D host for highly stable lithium–sulfur batteries. *Angew Chem Int Ed*. 2020;59(29):12129–12138.
101. Zhang Q, Wang Y, Seh ZW, Fu Z, Zhang R, Cui Y. Understanding the anchoring effect of two-dimensional layered materials for lithium–sulfur batteries. *Nano Lett*. 2015;15(6):3780–3786.
102. Chen X, Peng H-J, Zhang R, et al. An analogous periodic law for strong anchoring of polysulfides on polar hosts in lithium sulfur batteries: S- or Li-binding on first-row transition-metal sulfides? *ACS Energy Lett*. 2017;2(4):795–801.
103. Song X, Qu Y, Zhao L, Zhao M. Monolayer  $\text{Fe}_3\text{GeX}_2$  ( $X = \text{S}, \text{Se}$ , and Te) as highly efficient electrocatalysts for lithium–sulfur batteries. *ACS Appl Mater Interfaces*. 2021;13(10):11845–11851.
104. Xu Y, Ou X, Zhang X. Theoretical study of two-dimensional  $\alpha$ -Tellurene with pseudo-heterospecies as a promising elemental anchoring material for lithium–sulfur batteries. *J Phys Chem C*. 2021;125(8):4623–4631.
105. Wang P, Xi B, Zhang Z, Huang M, Feng J, Xiong S. Atomic tungsten on graphene with unique coordination enabling kinetically boosted lithium–sulfur batteries. *Angew Chem Int Ed*. 2021;60(28):15563–15571.
106. Pang Q, Kundu D, Cuisinier M, Nazar LF. Surface-enhanced redox chemistry of polysulphides on a metallic and polar host for lithium–sulphur batteries. *Nat Commun*. 2014;5(1):4759.
107. Chen C-Y, Peng H-J, Hou T-Z, et al. A quinonoid-imine-enriched nanostructured polymer mediator for lithium–sulfur batteries. *Adv Mater*. 2017;29(23):1606802.
108. Zhang Z-W, Peng H-J, Zhao M, Huang JQ. Heterogeneous/homogeneous mediators for high-energy-density lithium–sulfur batteries: progress and prospects. *Adv Funct Mater*. 2018;28(38):1707536.
109. Liu Z, Zhou L, Ge Q, et al. Atomic iron catalysis of polysulfide conversion in lithium–sulfur batteries. *ACS Appl Mater Interfaces*. 2018;10(23):19311–19317.
110. Shen J, Wang Z, Xu X, et al. Surface/interface structure and chemistry of lithium–sulfur batteries: from density functional theory calculations' perspective. *Adv Energy Sustain Res*. 2021;2(6):2100007.
111. Assary RS, Curtiss LA, Moore JS. Toward a molecular understanding of energetics in Li–S batteries using nonaqueous electrolytes: a high-level quantum chemical study. *J Phys Chem C*. 2014;118(22):11545–11558.
112. Shao Q, Lu P, Xu L, et al. Rational design of  $\text{MoS}_2$  nanosheets decorated on mesoporous hollow carbon spheres as a dual-functional accelerator in sulfur cathode for advanced pouch-type Li–S batteries. *J Energy Chem*. 2020;51:262–271.
113. Zhou J, Zhou X, Sun Y, Shen X, Qian T, Yan C. Insight into the reaction mechanism of sulfur chains adjustable polymer cathode for high-loading lithium–organosulfur batteries. *J Energy Chem*. 2021;56:238–244.
114. Wang C, Sun L, Li K, Wu Z, Zhang F, Wang L. Unravel the catalytic effect of two-dimensional metal sulfides on polysulfide conversions for lithium–sulfur batteries. *ACS Appl Mater Interfaces*. 2020;12(39):43560–43567.
115. Guo J, Jiang H, Li X, et al. Defective graphene coating-induced exposed interfaces on  $\text{CoS}$  nanosheets for high redox electrocatalysis in lithium–sulfur batteries. *Energy Storage Mater*. 2021;40:358–367.
116. Xu J, Yang L-K, Cao S-F, et al. Sandwiched cathodes assembled from  $\text{CoS}_2$ -modified carbon clothes for high-performance lithium–sulfur batteries. *Adv Sci*. 2021;8(16):2101019.
117. Lee JS, Kim W, Jang J, Manthiram A. Sulfur-embedded activated multichannel carbon nanofiber composites for long-life, high-rate lithium–sulfur batteries. *Adv Energy Mater*. 2017;7(5):1601943.
118. Su Z, Chen M, Pan Y, et al. Expediting polysulfide catalytic conversion for lithium–sulfur batteries via in situ implanted ultrafine  $\text{Fe}_3\text{O}_4$  nanocrystals in carbon nanospheres. *J Mater Chem A*. 2020;8(45):24117–24127.
119. Zhou J, Liu X, Zhu L, et al. Deciphering the modulation essence of  $p$  bands in Co-based compounds on Li–S chemistry. *Joule*. 2018;2(12):2681–2693.

120. Shen J, Xu X, Liu J, et al. Mechanistic understanding of metal phosphide host for sulfur cathode in high-energy-density lithium–sulfur batteries. *ACS Nano*. 2019;13(8):8986-8996.
121. Shen Z, Cao M, Zhang Z, et al. Efficient Ni<sub>2</sub>Co<sub>4</sub>P<sub>3</sub> nanowires catalysts enhance ultrahigh-loading lithium–sulfur conversion in a microreactor-like battery. *Adv Funct Mater*. 2020;30(3):1906661.
122. Shen J, Xu X, Liu J, et al. Unraveling the catalytic activity of Fe-based compounds toward Li<sub>2</sub>S<sub>x</sub> in Li–S chemical system from *d*-*p* bands. *Adv Energy Mater*. 2021;11(26):2100673.
123. Hammer B, Norskov JK. Why gold is the noblest of all the metals. *Nature*. 1995;376(6537):238-240.
124. Chang K, Mei Z, Wang T, Kang Q, Ouyang S, Ye J. MoS<sub>2</sub>/graphene cocatalyst for efficient photocatalytic H<sub>2</sub> evolution under visible light irradiation. *ACS Nano*. 2014;8(7):7078-7087.
125. Kibsgaard J, Chen Z, Reinecke BN, Jaramillo TF. Engineering the surface structure of MoS<sub>2</sub> to preferentially expose active edge sites for electrocatalysis. *Nat Mater*. 2012;11(11):963-969.
126. Kiriya D, Lobaccaro P, Nyein HYY, et al. General thermal texturization process of MoS<sub>2</sub> for efficient electrocatalytic hydrogen evolution reaction. *Nano Lett*. 2016;16(7):4047-4053.
127. Asadi M, Kumar B, Behranginia A, et al. Robust carbon dioxide reduction on molybdenum disulphide edges. *Nat Commun*. 2014;5(1):4470.
128. Asadi M, Kumar B, Liu C, et al. Cathode based on molybdenum disulfide nanoflakes for lithium–oxygen batteries. *ACS Nano*. 2016;10(2):2167-2175.
129. Wang T, Gao D, Zhuo J, et al. Size-dependent enhancement of electrocatalytic oxygen-reduction and hydrogen-evolution performance of MoS<sub>2</sub> particles. *Chem Eur J*. 2013;19(36):11939-11948.
130. Lin H, Yang L, Jiang X, et al. Electrocatalysis of polysulfide conversion by sulfur-deficient MoS<sub>2</sub> nanoflakes for lithium–sulfur batteries. *Energ Environ Sci*. 2017;10(6):1476-1486.
131. Yang Y, Yu Y, Ma G, et al. High-performance lithium–sulfur batteries fabricated from a three-dimensional porous reduced graphene oxide/La<sub>2</sub>O<sub>3</sub> microboards/sulfur aerogel. *Ceram Int*. 2019;45(7):9017-9024.
132. Zhang X, Chen M, Zhang Q, Liu J, Wu Y. New insights into synergistic effects of La<sub>2</sub>O<sub>3</sub> and nitrogen doped carbon for improved redox kinetics in lithium–sulfur batteries: a computational study. *Appl Surf Sci*. 2021;563:150172.
133. Liu Y-T, Zhu X-D, Pan L. Hybrid architectures based on 2D MXenes and low-dimensional inorganic nanostructures: methods, synergies, and energy-related applications. *Small*. 2018;14(51):1803632.
134. Li B, Xu H, Ma Y, Yang S. Harnessing the unique properties of 2D materials for advanced lithium–sulfur batteries. *Nanoscale Horiz*. 2019;4(1):77-98.
135. Xiao Z, Li Z, Meng X, Wang R. MXene-engineered lithium–sulfur batteries. *J Mater Chem A*. 2019;7(40):22730-22743.
136. Wang D, Li F, Lian R, et al. A general atomic surface modification strategy for improving anchoring and electrocatalysis behavior of Ti<sub>3</sub>C<sub>2</sub>T<sub>2</sub> MXene in lithium–sulfur batteries. *ACS Nano*. 2019;13(10):11078-11086.
137. Zhang Q, Xiao Y, Fu Y, et al. Theoretical prediction of B/Al-doped black phosphorus as potential cathode material in lithium–sulfur batteries. *Appl Surf Sci*. 2020;512:145639.
138. Liu J, Xiao S, Chang L, et al. Regulating the *d* band in WS<sub>2</sub>@NC hierarchical nanospheres for efficient lithium polysulfide conversion in lithium–sulfur batteries. *J Energy Chem*. 2021;56:343-352.
139. Han Z, Zhao S, Xiao J, et al. Engineering *d*-*p* orbital hybridization in single-atom metal-embedded three-dimensional electrodes for Li–S batteries. *Adv Mater*. 2021;33(44):2105947.
140. Zhao Z, Yi Z, Li H, et al. Synergetic effect of spatially separated dual co-catalyst for accelerating multiple conversion reaction in advanced lithium sulfur batteries. *Nano Energy*. 2021;81:105621.
141. Li X, Li X, Banis MN, et al. Tailoring interactions of carbon and sulfur in Li–S battery cathodes: significant effects of carbon–heteroatom bonds. *J Mater Chem A*. 2014;2(32):12866-12872.
142. Urban A, Seo D-H, Ceder G. Computational understanding of Li-ion batteries. *npj Comput Mater*. 2016;2(1):16002.
143. Zhang H, Wang Z, Ren J, Liu J, Li J. Ultra-fast and accurate binding energy prediction of shuttle effect-suppressive sulfur hosts for lithium–sulfur batteries using machine learning. *Energy Storage Mater*. 2021;35:88-98.
144. Zhou G, Zhao S, Wang T, et al. Theoretical calculation guided design of single-atom catalysts toward fast kinetic and long-life Li–S batteries. *Nano Lett*. 2020;20(2):1252-1261.
145. Lian Z, Yang M, Jan F, Li B. Machine learning derived blueprint for rational design of the effective single-atom cathode catalyst of the lithium–sulfur battery. *J Phys Chem Lett*. 2021;12(29):7053-7059.
146. Zhang H, Wang Z, Cai J, Wu S, Li J. Machine-learning-enabled tricks of the trade for rapid host material discovery in Li–S battery. *ACS Appl Mater Interfaces*. 2021;13(45):53388-53397.
147. Gong S, Xie T, Zhu T, et al. Predicting charge density distribution of materials using a local-environment-based graph convolutional network. *Phys Rev B*. 2019;100(18):184103.
148. Xie T, Grossman JC. Crystal graph convolutional neural networks for an accurate and interpretable prediction of material properties. *Phys Rev Lett*. 2018;120(14):145301.
149. Sun W, Zheng Y, Yang K, et al. Machine learning-assisted molecular design and efficiency prediction for high-performance organic photovoltaic materials. *Sci Adv*. 2019;5(11):eaay4275.

## AUTHOR BIOGRAPHIES



**Shuai Feng** received her bachelor's degree from Ludong University in 2004, her master's degree from Shandong Normal University in 2007, and her Ph.D. from the Beijing Institute of Technology in 2016. She is currently an associate professor at College of chemistry and chemical engineering, Taishan University, and a visiting scholar at Tsinghua University. Her current research focuses on the catalytic mechanism of sulfur reduction reaction for host material in lithium–sulfur batteries.



**Xiang Chen** gained his bachelor's and Ph.D. degrees from the Department of Chemical Engineering at Tsinghua University in 2016 and 2021, respectively. He is currently a Shuimu Tsinghua Scholar at Tsinghua University. His research interests focus on understanding the chemical mechanism and materials science in rechargeable batteries

mainly through multi-scale simulations and machine learning.



**Qiang Zhang** received his bachelor's and Ph.D. degrees from Tsinghua University in 2004 and 2009, respectively. After a stay at Case Western Reserve University in the United States and the Fritz Haber Institute of the Max Planck Society in Germany, he joined Tsinghua University in 2011. He held the Newton Advanced Fellowship from the Royal Society and the National Science Fund for Distinguished Young Scholars. His current research interests are advanced energy materials, including Li metal anodes, solid-state electrolytes, Li–S batteries, and electrocatalysts.

**How to cite this article:** Feng S, Fu Z-H, Chen X, Zhang Q. A review on theoretical models for lithium–sulfur battery cathodes. *InfoMat*. 2022; 4(3):e12304. doi:10.1002/inf2.12304